UNIVERSIDAD AUTÓNOMA DE SAN LUIS POTOSÍ

FACULTAD DE CIENCIAS QUÍMICAS

PROGRAMA DE POSGRADO EN CIENCIAS EN BIOPROCESOS

LA ORGANOGELACIÓN DE ÉSTERES ALIFÁTICOS CONSTITUTIVOS DE BIOCERAS COMESTIBLES

ARTÍCULO DE INVESTIGACIÓN PARA
OBTENER EL GRADO DE:

DOCTOR EN CIENCIAS EN BIOPROCESOS

PRESENTA:

M.C. GILDA AVENDAÑO VÁSQUEZ

DIRECTOR DE TESIS:

DR. JORGE FERNANDO TORO VAZQUEZ

SAN LUIS POTOSÍ, S. L. P. SEPTIEMBRE 2020

UNIVERSIDAD AUTÓNOMA DE SAN LUIS POTOSÍ

FACULTAD DE CIENCIAS QUÍMICAS

PROGRAMA DE POSGRADO EN CIENCIAS EN BIOPROCESOS

LA ORGANOGELACIÓN DE ÉSTERES ALIFÁTICOS CONSTITUTIVOS DE BIOCERAS COMESTIBLES

ARTÍCULO DE INVESTIGACIÓN PARA
OBTENER EL GRADO DE:

DOCTOR EN CIENCIAS EN BIOPROCESOS

PRESENTA:

M.C. GILDA AVENDAÑO VÁSQUEZ

SINODALES:

DR. JORGE FERNANDO TORO VAZQUEZ

DRA. ELENA DIBILDOX ALVARADO

DR. JAIME DAVID PÉREZ MARTÍNEZ

DR. ALEJANDRO ROCHA URIBE

DR. ALBERTO GALLEGOS INFANTE

SAN LUI S POTOSÍ, S. L. P. SEPTIEMBRE 2020

Proyecto realizado en:

Laboratorio de Fisicoquímica de Alimentos del
Centro de Investigación y Estudios de Posgrado
Facultad de Ciencias Químicas

Universidad Autónoma de San Luis Potosí

Con financiamiento de:

Consejo Nacional de Ciencia y Tecnología (CONACyT)

Número de registro 301194/228501

La presente investigación fue financiada por el CONACYT con el proyecto CB-280981-2018.

El programa de Doctorado en Ciencias en Bioprocesos de la
Universidad Autónoma de San Luis Potosí
Pertenece al Programa Nacional de Posgrados de Calidad (PNPC) del
CONACyT, con número de registro 000590, en el Nivel Doctorado
(Consolidado).

Agradecimientos Académicos

Al Dr. Jorge F. Toro Vazquez, director del proyecto, por haberme dado la oportunidad de colaborar en su equipo de trabajo, compartir sus conocimientos y por el apoyo constante para cumplir este objetivo.

Al Dr. Jaime David Pérez Martínez, Dra. Elena Dibildox Alvarado, y M.C. Miriam Charó Alonso, por su apoyo e invaluables contribuciones durante el desarrollo de este proyecto y en mi crecimiento personal.

A la Dra. Flor de María Álvarez Mitre, Ing. Marisol Dávila Martínez, MC. María Eugenia Charó Alvarado, Dra. Anaid de la Peña Gil y Dr. Juan Ángel Morales Rueda. Por su ayuda en la capacitación y desarrollo de técnicas analíticas, como parte fundamental en el desarrollo de este proyecto.

Al CIESAS- CONACYT, por el apoyo financiero.

Agradecimientos Personales

A Dios, por permitirme llegar, sé que me escuchas. Y que me has colmado de bendiciones como mis padres (Hery y Mode) y mis hermanos (Leo y Nahun), gracias por apoyarme tanto.

A mi esposo y mi shapy. La paciencia es una virtud que sin duda ambos han desarrollado en el transcurso de su convivencia conmigo. Los amo.

A todos quienes fueron mis compañeros de laboratorio.

ÍNDICE

Artículo

El autoensamble de ésteres alquílicos simétricos y asimétricos en estado puro y en oleogeles.

Self-assembly of symmetrical and asymmetrical alkyl esters in the neat state and in edible oleogels

Self-assembly of symmetrical and asymmetrical alkyl esters in the neat state and in oleogels

Abstract

Saturated alkyl esters play an important role in determining the functional properties of the vegetable waxes used in the formulations of natural cosmetics and edible oleogels. We studied the relationship between the thermo-mechanical properties and crystal microstructure developed by saturated symmetrical (SE: 14:14, 16:16, 18:18, 20:20, and 22:22) and asymmetrical (AE: 18:14, 18:16, 18:20, 18:22) esters in the neat state and in oleogels. Additionally, we evaluated the effect of 1-stearoyl-glycerol (MSG; 0.5% and 1%) in the development of SE and AE oleogels. The X-ray and microscopy analysis in the neat state showed that SE self-assembled developing plate-like crystals, while AE developed acicular-like crystals. Microscopy analysis indicated that AE and SE followed similar crystallization behavior in the oleogels. The AE oleogels had higher elasticity (*G'*) than the SE oleogels. In both types of oleogels as the ester carbon number increased the oleogels' *G'* decreased and crystal size increased. The addition of just 0.5% MSG, particularly in the AE oleogels, limited the decrease in *G'* as the ester carbon number increased, mainly because MSG decreased crystal size. The calorimetry results suggested that during cooling the MSG and the alkyl esters developed a co-crystal. Nevertheless, part of the MSG did not interact with the ester molecules and crystallized independently. These MSG crystals acted as active fillers of the microstructure formed by the co-crystals. The overall effect was that in comparison with the alkyl ester oleogels the alkyl ester oleogels with 0.5% and 1% MSG had higher *G'* with frequency independent rheological behavior. This rheological behavior was particularly evident with the AE oleogels. Therefore, ester composition and molecular structure (i.e., symmetry or asymmetry) greatly influence its molecular self-assembly and subsequently the oleogels' thermomechanical properties. Studies using molecular mechanics modeling are underway to establish the mechanism for AE and SE self-

assembly with and without MSG. The overall goal is to understand and control the crystallization of vegetable waxes for the development of functional edible oleogels.

El autoensamble de ésteres alquílicos simétricos y asimétricos en estado puro y en oleogeles

Resumen

Los ésteres alquílicos saturados juegan un papel importante en la determinación de las propiedades funcionales de las ceras vegetales utilizadas en las formulaciones de cosméticos naturales y oleogeles comestibles. Estudiamos la relación entre las propiedades termomecánicas y la microestructura cristalina desarrollada por esteres saturados simétricos (SE: 14:14, 16:16, 18:18, 20:20 y 22:22) y asimétricos (AE: 18: 14, 18:16, 18:20, 18:22) en estado puro y en oleogeles. Además, evaluamos el efecto del 1-estearoil-glicerol (MSG; 0.5% y 1%) en el desarrollo de oleogeles SE y AE. El análisis por rayos X y microscopía mostró que en estado puro y en los oleogeles los SE se auto-ensamblan desarrollando cristales en forma de placas, mientras que AE desarrollaron cristales aciculares. Los análisis de microscopía mostraron que AE y SE siguen un comportamiento de cristalización similar en los oleogeles. Los oleogeles AE tuvieron mayor elasticidad (*G'*) que los oleogeles SE. En ambos tipos de oleogeles a medida que aumentaba el número de carbonos del éster, *G'* de los oleogeles disminuía mientras el tamaño del cristal aumentaba. La adición de solo 0.5% de MSG, particularmente en los oleogeles AE, limitó la disminución de *G'* a medida que aumentaba el número de carbono del éster, principalmente porque MSG disminuye el tamaño del cristal. Los resultados de calorimetría sugieren que durante el enfriamiento el MSG y los esteres alquílicos desarrollan un co-cristal. Sin embargo, parte del MSG no interactuó con las moléculas de éster y cristalizó de manera independiente. Estos cristales de MSG actuaron como relleno de la microestructura formada por los co-cristales. El efecto general fue que en comparación con los oleogeles de éster alquílico, los oleogeles de éster alquílico con 0.5 y 1.0% mantienen un *G'* elevado con un comportamiento reológico independiente de la frecuencia. Este comportamiento reológico fue particularmente evidente con los oleogeles de AE. Estos resultados

mostraron que la composición del éster y la estructura molecular (es decir, simetría o asimetría) influyen en gran medida en su autoensamblaje molecular y, posteriormente, en las propiedades termomecánicas de los oleogeles. Se están realizando estudios que utilizan modelos de mecánica molecular para establecer el mecanismo que siguen AE y SE en su autoensamblaje con y sin MSG. El objetivo general es comprender y controlar la cristalización de las ceras vegetales en el desarrollo de oleogeles comestibles funcionales.

F

Frontiers In Sustainable Food Systems Editorial Office <sustainablefood systems.editorial.office@frontiersin.org>
Vie 24/07/2020 10:49 AM
Para: Usted

Dear Dr Avendaño-Vásquez,

Frontiers In Sustainable Food Systems Editorial Office has sent you a message. Please click 'Reply' to send a direct response

I am pleased to inform you that your manuscript Self-assembly of symmetrical and asymmetrical alkyl esters in the neat state and in edible oleogels has been approved for production and accepted for publication in Frontiers in Sustainable Food Systems, section Sustainable Food Processing.
Your manuscript is currently being prepared for publication. The provisional version of the abstract or introductory section is currently available online. Please do not communicate any changes at this stage. You will be contacted as soon as the author proofs are ready for your revisions.

Manuscript title: Self-assembly of symmetrical and asymmetrical alkyl esters in the neat state and in edible oleogels
Journal: Frontiers in Sustainable Food Systems, section Sustainable Food Processing
Article type: Original Research
Authors: Gilda Avendaño-Vásquez, Anaid De La Peña-Gil, Maria E. Charó-Alvarado, Miriam A Charó-Alonso, Jorge F Toro-Vazquez
Manuscript ID: 550563
Edited by: Miguel Cerqueira

Due to lockdown orders in various countries you may experience a delay in the production and publication of your article but please be assured that we are working to provide them as soon as possible and ask for your patience.

You can click here to access the final review reports and manuscript: http://www.frontiersin.org/Review/EnterReviewForum.aspx?activationno=8172b1b9-2642-433a-866a-22624fa042cb

As an author, it is important that you maintain your Frontiers research network (Loop) profile up to date, as your publication will be linked to your profile allowing you and your publications to be more discoverable. You can update profile pages (profile pictures, short bio, list of publications) using this link: http://loop.frontiersin.org/people/

Tell us what you think!

At Frontiers we are constantly trying to improve our Collaborative Review process and would like to get your feedback on how we did. Please complete our short 3-minute survey and we will donate $1 to Enfants du Monde, a Swiss non-profit organization: https://frontiers.qualtrics.com/jfe/form/SV_8q8kYmXRvxBH5at?survey=author&aid=550563&uid=

Thank you very much for taking the time to share your thoughts.

Best regards,

Frontiers in Sustainable Food Systems

Frontiers | Editorial Office - Collaborative Peer Review Team
www.frontiersin.org

12 Moorgate, London EC2R 6DA – United Kingdom
Office T 44 203 5144 082

For technical issues, please contact our IT Helpdesk (support@frontiersin.org) or visit our Frontiers Help Center (zendesk.frontiersin.org/hc/en-us)

https://www.frontiersin.org/register

frontiers in Sustainable Food Systems | Sustainable Food Processing

ORIGINAL RESEARCH ARTICLE
Front. Sustain. Food Syst. | doi: 10.3389/fsufs.2020.00132

Self-assembly of symmetrical and asymmetrical alkyl esters in the neat state and in oleogels

Gilda Avendaño-Vásquez[1], Anaid De La Peña-Gil[1], Maria E. Charó-Alvarado[2], Miriam A. Charó-Alonso[2] and Jorge F. Toro-Vazquez[1]*

[1]Facultad de Ciencias Químicas, Universidad Autónoma de San Luis Potosí, Mexico

Saturated alkyl esters play an important role in determining the functional properties of the vegetable waxes used in the formulations of natural cosmetics and edible oleogels. We studied the relationship between the thermo-mechanical properties and crystal microstructure developed by saturated symmetrical (SE: 14:14, 16:16, 18:18, 20:20, and 22:22) and asymmetrical (AE: 18:14, 18:16, 18:20, 18:22) esters in the neat state and in oleogels. Additionally, we evaluated the effect of 1-stearoyl-glycerol (MSG; 0.5% and 1%) in the development of SE and AE oleogels. The X-ray and microscopy analysis in the neat state showed that SE self-assembled developing plate-like crystals, while AE developed acicular-like crystals. Microscopy analysis indicated that AE and SE followed similar crystallization behavior in the oleogels. The AE oleogels had higher elasticity (G') than the SE oleogels. In both types of oleogels as the ester carbon number increased the oleogels' G' decreased and crystal size increased. The addition of just 0.5% MSG, particularly in the AE oleogels, limited the decrease in G' as the ester carbon number increased, mainly because MSG decreased crystal size. The calorimetry results suggested that during cooling the MSG and the alkyl esters developed a co-crystal. Nevertheless, part of the MSG did not interact with the ester molecules and crystallized independently. These MSG crystals acted as active fillers of the microstructure formed by the co-crystals. The overall effect was that in comparison with the alkyl ester oleogels the alkyl ester oleogels with 0.5% and 1% MSG had higher G' with frequency independent rheological behavior. This rheological behavior was particularly evident with the AE oleogels. Therefore, ester composition and molecular structure (i.e., symmetry or asymmetry) greatly influence its molecular self-assembly and subsequently the oleogels' thermo-mechanical properties. Studies using molecular mechanics modeling are underway to establish the mechanism for AE and SE self-assembly with and without MSG. The overall goal is to understand and control the crystallization of vegetable waxes for the development of functional edible oleogels.

Keywords: Oleogels, alkyl esters, Monoglycerides, Vegetable wax, Cosmetics, Co-crystals

Received: 09 Apr 2020; **Accepted:** 24 Jul 2020.

* **Correspondence:** Mx. Jorge F. Toro-Vazquez, Facultad de Ciencias Químicas, Universidad Autónoma de San Luis Potosí, SAN LUIS POTOSI, Mexico, toro@uaslp.mx

Self-assembly of symmetrical and asymmetrical alkyl esters in the neat state and in oleogels

Avendaño-Vásquez G., De la Peña-Gil A., Charó-Alvarado M. E., Charó-Alonso M. A., Toro-Vazquez, J. F.[a]

Facultad de Ciencias Químicas-CIEP, Universidad Autónoma de San Luis Potosí, México

[a] Corresponding author
Facultad de Ciencias Químicas-CIEP
Laboratorio de Fisicoquímica de Alimentos
Av. Dr. Manuel Nava 6
Zona Universitaria
San Luis Potosí, SLP 78210
Phone 52-444-8262300 Ext. 6555

KEYWORDS: Oleogels, Alkyl Esters, Monoglycerides, Vegetable wax, Cosmetics, Co-crystals

NUMBER OF WORDS: 780
NUMBER OF FIGURES: 13
NUMBER OF TABLES: 1

Abstract

Saturated alkyl esters play an important role in determining the functional properties of the vegetable waxes used in the formulations of natural cosmetics and edible oleogels. We studied the relationship between the thermo-mechanical properties and crystal microstructure developed by saturated symmetrical (SE: 14:14, 16:16, 18:18, 20:20, and 22:22) and asymmetrical (AE: 18:14, 18:16, 18:20, 18:22) esters in the neat state and in oleogels. Additionally, we evaluated the effect of 1-stearoyl-glycerol (MSG; 0.5% and 1%) in the development of SE and AE oleogels. The X-ray and microscopy analysis in the neat state showed that SE self-assembled developing plate-like crystals, while AE developed acicular-like crystals. Microscopy analysis indicated that AE and SE followed similar crystallization behavior in the oleogels. The AE oleogels had higher elasticity (*G'*) than the SE oleogels. In both types of oleogels as the ester carbon number increased the oleogels' *G'* decreased and crystal size increased. The addition of just 0.5% MSG, particularly in the AE oleogels, limited the decrease in *G'* as the ester carbon number increased, mainly because MSG decreased crystal size. The calorimetry results suggested that during cooling the MSG and the alkyl esters developed a co-crystal. Nevertheless, part of the MSG did not interact with the ester molecules and crystallized independently. These MSG crystals acted as active fillers of the microstructure formed by the co-crystals. The overall effect was that in comparison with the alkyl ester oleogels the alkyl ester oleogels with 0.5% and 1% MSG had higher *G'* with frequency independent rheological behavior. This rheological behavior was particularly evident with the AE oleogels. Therefore, ester composition and molecular structure (i.e., symmetry or asymmetry) greatly influence its molecular self-assembly and subsequently the oleogels' thermomechanical properties. Studies using molecular mechanics modeling are underway to establish the mechanism for AE and SE self-assembly with and without MSG. The overall goal is to understand and control the crystallization of vegetable waxes for the development of functional edible oleogels.

1. INTRODUCTION

Several molecules of low molecular weight (< 3000 Da) at temperatures below their solubility limit in an organic solvent (i.e., vegetable oil), have the capability of self-assembly. Through this process lipophilic or amphiphilic molecules like phytosterols (Bot and Agterof, 2006; Bot et al., 2008, 2009), lecithin (Han et al., 2014; Martínez-Ávila et al., 2019), monoglycerides (Chen et al., 2009; López-Martínez et al., 2014), (R)-12-hydroxystearic acid (Rogers and Marangoni, 2008; Lam and Rogers, 2011; Abraham et al., 2012; Co and Marangoni, 2013), *n*-alkanes, long chain alkyl esters, fatty acids and fatty alcohols (Gandolfo et al., 2004; Morales-Rueda et al., 2009; Lam and Rogers, 2011; Co and Marangoni, 2013; Sagiri et al., 2015) form three-dimensional crystal structures that physically trap vegetable oils providing them with viscoelastic and thermoreversible properties (Toro-Vazquez and Pérez-Martínez, 2018).

Several studies have shown that this process (i.e., organogelation) is a useful and novel alternative to structure vegetable oils for food systems without the use of *trans* and/or saturated fats (Dassanayake et al., 2011; Marangoni and Garti, 2011; Co and Marangoni, 2012; Rogers et al., 2014). Nowadays, the food industry faces the need to develop thermodynamically stable systems with functional properties accepted by the consumers without the use of *trans* and saturated fatty acids. This is due to the well-documented negative effect of the saturated and *trans* fats on cardiovascular health. One of the most promising alternatives for the development of edible gelled systems (i.e., oleogels) is the use of natural vegetable waxes (Blake et al., 2018). Additionally, the major cosmetic companies are moving away from animal-based (e. g., tallow) and petroleum derived materials (e. g., petroleum jelly), looking now for renewable and functional vegetable-based materials. We can also develop vegetable waxes-based oleogels with useful and novel functional properties for the cosmetics' industry (Ferrari and Mondet, 2003; Morales et al., 2010; Perez Nowak, 2012). The use of vegetable waxes is the current natural trend for the development of natural cosmetics, e.g., organic cosmetics (Cosmetic Lab, 2016; Fórmula Botánica, 2019).

Most of the vegetable waxes already in the commercial market are characterized by their high content of long chain saturated alkyl esters (i.e., greater than 60%). In other waxes a different lipid-like compound is the major component (i.e., *n*-alkanes) and the alkyl esters is a minor but still a significant component fraction (between 6% and 16%) (Blake et al., 2018). In any case, the alkyl esters in the vegetable waxes are essentially constituted by saturated long chain fatty acids between 16 and 32 carbon atoms (Doan et al., 2017), which provide the waxes with a solid texture at room temperature. Exception to this is the liquid wax obtained from jojoba (*Simmondsia chinensis*) seeds composed by nearly 97% of esters constituted by heneicosanoic acid (21:0), behenic acid (22:0), and particularly 13, 16 docosadienoic acid (22:2), and fatty alcohols of 20, 22 and 24 carbons with one double bond (*cis*-11-eicosenol, *cis*-13-docosenol, and *cis*-15- tetracosenol) (Busson-Breysse et al., 1994; Ghamdi et al., 2017). Thus, the alkyl ester content is often used to explain the crystallization and melting behavior of the vegetable waxes in the neat state and in the development of oleogels. Within this context, rice bran and sunflower waxes are considered chemically homogeneous given their high alkyl ester content (92%-100%) and low compositional heterogeneity (i.e., less than 6% of free alkyl acids and free alkyl alcohols) (Doan et al., 2017). These two vegetable waxes crystallize as one single narrow exotherm, developing large needle-like crystals with high melting entropy values. In contrast, carnauba and candelilla wax with lower concentration of their main component (i.e., carnauba wax with 62% to 85% of alkyl esters and candelilla wax with 45% to 65% of *n*-alkanes) have higher heterogeneous composition. In consequence, the carnauba and the candelilla wax crystallize showing broader exotherms with multiple peaks developing small dendritic crystals or microplatelets, respectively, with lower melting entropy. This is particularly evident with candelilla wax that shows the higher compositional heterogeneity with just 6% to 16% of alkyl esters (Alvarez-Mitre et al., 2012; Blake et al., 2014; Doan et al., 2017).

From the above, it is evident that the alkyl esters play an important role in the physical properties showed by vegetable waxes. Nevertheless, there is limited information

about their physical properties either in the pure state or in oleogels. Within this context the main objective of this study was to investigate the relationship between the thermomechanical properties and crystal microstructure developed by saturated alkyl esters in the neat state and in oleogels. This, using pure alkyl esters constituted by saturated fatty acids and fatty alcohols with the same number of carbons [symmetrical esters; myristyl myristate (14:14), palmityl palmitate (16:16), stearyl stearate (18:18), arachidyl arachidate (20:20) and behenyl behenate (22:22)] and with different number of carbon [asymmetrical esters; stearyl myristate (18:14), stearyl palmitate (18:16), stearyl arachidate (18:20), and stearyl behenate (18:22)].

On the other hand, studies done by different research groups had shown that the crystallization behavior of vegetable waxes (i.e., crystal size and shape) and further development of the crystal network are affected by other components, naturally present in the wax or intentionally added (Toro-Vazquez et al., 2007; Morales-Rueda et al., 2009; Blake et al., 2014; Chopin-Doroteo et al. 2011; Dassanayake et al., 2009; Hwang et al., 2014; Rocha-Amador et al., 2014). Monoglycerides are a minor component commonly present in refined vegetable oils at low concentrations commonly between 0.05% and 0.2% (Gunstone, 2002). Because their amphiphilic character and capability of developing hydrogen bonds when added to vegetable oils the monoglycerides are able to develop emulsions and oleogels (Ojijo et al., 2004; Chen et al., 2009; López-Martínez et al., 2014; Marangoni and Garti, 2018). Therefore, monoglycerides play an important role in the development and stability of organogelled emulsions (Toro-Vazquez et al., 2013). In these systems the monoglycerides might affect the self-assembly of alkyl esters present in vegetable waxes. Thus, a second objective of this study was to investigate the effect of intentionally added monoglycerides (0.5% and 1%) in the self-assembly of alkyl esters during the formation of oleogels.

2. MATERIALS AND METHODS

2.1. MATERIALS

Refined, bleached and deodorized high oleic safflower oil was obtained from a local distributor (Coral International, San Luis Potosi, Mexico). The high oleic safflower oil was used as the liquid phase in the development of oleogels. As previously determined by HPLC the major triacylglyceride in the vegetable oil was OOO (65.65% ± 0.15%), followed by LOO (16.26% ± 0.04), and POO (8.58% ± 0.04), and minor concentrations of StOO (2.64% ± 0.01%), LLO (2.25% ± 0.02%), POL (1.70% + 0.11), StLL (0.87% ± 0.05%), and LLL (0.46% ± 0.01%) (O = oleic acid; L = linoleic acid; St = stearic acid; P = palmitic acid) (Alvarez-Mitre et al., 2012). Analytical grade 1-stearoyl-*rac*-glycerol (MSG) with a purity > 99% was obtained from Sigma Aldrich (St. Louis, MO, USA). The linear alkyl esters with a purity > 99% were obtained from Nu-Check Prep, Inc. (Elysian, MN, USA) and were constituted by saturated fatty acids and saturated fatty alcohols with the same number of carbons (i.e., symmetrical esters, SE) or with different number of carbon (i.e., asymmetrical esters, AE). The SE were: tetradecyl tetradecanoate (myristyl myristate; 14:14), hexadecyl hexadecanoate (palmityl palmitate; 16:16), octadecyl octadecanoate (stearyl stearate; 18:18), eicosyl eicosanoate (arachidyl arachidate; 20:20), and docosanyl docosanoate (behenyl behenate; 22:22), and the AE were: octadecyl tetradecanoate (stearyl myristate; 18:14), octadecyl hexadecanoate (stearyl palmitate; 18:16), octadecyl eicosanoate (stearyl arachidate; 18:20), and octadecyl docosanoate (stearyl behenate; 18:22). The MSG and alkyl esters were stored under desiccant conditions (phosphorus pentoxide) at -20°C.

2.2. X-RAY MEASUREMENTS

Neat alkyl esters were initially heated at 160°C for 20 min, after that the samples were allowed to cool at room temperature followed by 24 h storage at -5°C. After this time the samples X-ray pattern, in a silicon crystal sample holder, were recorded at 5°C with

a Bruker D8 Advance diffractometer (CuKα-irradiation λ = 1.5406, high-rate detector Lynx Eye) equipped with a parallel beam geometry. Angular scans were obtained from 1° to 40° using a step size of 0.01° and a scan speed of 0.32°/s. Data processing and analyses were performed using DIFFRAC.EVA software (V 5.1, Bruker, Karlsruhe, Germany).

2.3. CRYSTALLIZATION AND MELTING BEHAVIOR OF ALKYL ESTERS

2.3.1. DIFFERENTIAL SCANNING CALORIMETRY OF NEAT ALKYL ESTERS

The crystallization and melting profile of the neat alkyl esters (SE and AE) were determined by differential scanning calorimetry (Q2000, TA Instruments; New Castle, DL, USA). The corresponding sample (≈5-7 mg) was sealed in aluminum pans, heated at 160°C for 20 min and then cooled to 10 °C/min until achieving - 5°C. After 2 min at this temperature the system was heated at 5 °C/min until achieving 160°C. The use of this time-temperature condition assured the full melting of all the alkyl esters studied, particularly those with the highest number of carbons (i.e., 20:20, 22:22). The crystallization and heating thermograms were determined with the equipment software by plotting the heat flux of the sample as a function of the temperature. Using the first derivative of the heat flux from the cooling thermogram we determined the temperature at the beginning of the crystallization exotherm (T_{Cr}), and the area below the corresponding exotherm (i.e., heat of crystallization; ΔH_{Cr}). From the heating thermogram we determined the temperature at the maximum of the heat flow of the endotherm (T_M), and the heat of melting (ΔH_M). For each alkyl ester we obtained two independent cooling and heating thermograms (n = 2).

2.3.2. FITTING OF THE HILDEBRAND EQUATION

We evaluated the ideal crystallization/melting behavior of the SE and AE through the Hildebrand equation (Hildebrand and Robert-Lane S., 1950),

$$\ln(x) = \frac{\Delta H_M}{R\left(\frac{1}{T_S} - \frac{1}{T_E}\right)} \qquad [1]$$

$$\frac{1}{T_s} = \frac{1}{T_E} + \frac{R[\ln(x)]}{\Delta H_M} \qquad [2]$$

where ΔH_M is the enthalpy of fusion per mole of the corresponding neat alky ester, T_E and T_S are the melting temperature of the neat alky ester and in the oil solutions (i.e., $T_S = T_M$; see section **2.3.1**), respectively, *X* is the mole fraction of the alkyl ester in the vegetable oil, and R is the universal gas constant. For this we prepared 500 mg of 0.5% to 5% alkyl esters solutions in safflower oil solutions in glass vials (12 mm x 35 mm). To solubilize the alkyl esters the vials were placed in an oven set to 100°C and heated during 15 min with intermittent 1 min gently mixing periods using a vortex mixer. The crystallization and heating thermograms for the alkyl esters solutions in safflower oil as described in section 2.3.1. However, in this case the sample was heated at 100°C for 20 min and then cooled to 10°C/min until achieving -5°C. After 2 min at this temperature the system was heated at 5°C/min until achieving 100°C. The corresponding thermal parameters were fitted to the Hildebrand equation determining the linear regression of Ln(*X*) on $1/T_S$ and comparing the ΔH_M for neat alkyl esters calculated with the fitting equation with the corresponding ΔH_M value determined experimentally. For each alkyl ester concentration of the SE and AE we did at least three independent determinations ($n \geq 3$).

2.3.3. EFFECT OF MSG IN THE THERMAL BEHAVIOR OF ALKYL ESTERS SOLUTIONS IN THE VEGETABLE OIL

To evaluate the MSG effect in the crystallization/melting behavior of the alkyl esters, we prepared 3% alkyl esters-MSG solutions containing 0%, 0.5% or 1% (wt/wt) of MSG. For this we prepared the corresponding 3% alkyl ester solution as indicated in section **2.3.2,** adding the corresponding proportion of MSG once the alkyl esters

solution achieved 80°C-85°C. Afterwards, the alkyl ester and alkyl ester-MSG solutions were stored at 5°C until their use. The crystallization and melting profile of the 3% alkyl esters-MSG solution were determined by differential scanning calorimetry. To evaluate the MSG effect in the crystallization and melting profile of the alkyl ester-MSG system, we determined also the cooling and heating thermograms for the 0.5% and 1% MSG solutions in safflower oil. For each of the alkyl esters-MSG systems studied we obtained two independent cooling and heating thermograms (n = 2).

2.4. RHEOLOGICAL MEASUREMENTS IN THE OLEOGELS

The storage (G') and loss (G'') modulus of the alkyl ester-MSG systems were measured with an Anton Paar MCR301 rheometer (Paar Physica MCR 301, Stuttgart, Germany) using a steel truncated cone plate geometry (CP25-1TG). A sample of a pre-heated (≈100°C) alkyl ester-MSG system was applied on the base of the rheometer geometry previously set at 100°C, and the cone was set using the true-gap function of the software. After 20 min at 100°C, the system was cooled at 10 °C/min until achieving -5°C. After 2 min at this temperature we applied a strain sweep between 0.001-100% using a frequency (ω) of 1 Hz. The G' and G" of the alkyl ester-MSG system were obtained from the linear viscoelastic region (strain between 0.002% and 0.03%). In a parallel experiment we determined the phase shift angle (δ) as a function of ω (-5°C; 100 Hz and 0.1 Hz) using a strain within the linear viscoelastic region. The sample temperature was controlled with a Peltier temperature control located on the base of the geometry and with a Peltier-controlled hood (H-PTD 200). The control of the equipment was made through the software Start Rheoplus US200/32 version 2.65 (Anton Paar, Graz, Austria). For each alkyl ester-MSG system we did two independent rheological measurements (n = 2).

2.5. POLARIZED LIGHT MICROSCOPY

Polarized light microphotographs (PLM) of the oleogels were obtained using a polarizing light microscope (Olympus BX51; Olympus Optical Co., Ltd., Tokyo, Japan) equipped with a color video camera (KP-D50; Hitachi Digital, Tokyo, Japan) and a heating/cooling stage (TP94; Linkam Scientific Instruments, Ltd., Surrey, England) connected to a temperature control station (LTS 350; Linkam Scientific Instruments, Ltd.) and a liquid nitrogen tank. A drop of the alkyl ester-MSG solution was applied on a glass slide and then set in the heating/cooling stage of the microscope. We applied the same time-temperature program as described in section 2.3, but here after arriving at a temperature 10°C above the corresponding T_{Cr} the sample was smear on the slide surface using another pre-heated glass slide at a 45° angle. Then, the stage was closed and the cooling continued until achieving -5°C. PLM of the corresponding microstructure were obtained after two minutes at this temperature.

2.5. STATISTICAL ANALYSIS

The treatment conditions studied (i.e., type of alkyl ester, concentration of MSG) were analyzed by ANOVA and contrast between the treatment means. For the data obtained in section 2.3.2, the thermal parameters were fitted to the Hildebrand equation by linear regression. In all cases the software used was STATISTICA V 12 (StatSoft Inc., Tulsa, OK).

3. RESULTS AND DISCUSSION

3.1. X-RAY DIFFRACTION AND THERMAL BEHAVIOR OF NEAT ALKYL ESTERS

The corresponding lattice spacings (*d*, Å) and calculated extended molecular lengths (*L*, Å) for the neat SE and AE are summarized in Table 1. As stated in the Materials

and Methods section, the SE and AE oleogels studied were developed and characterized at -5°C while the X-ray analysis of the neat alkyl esters was done at 5°C. Unfortunately the diffractometer could not control the temperature below 5°C. However, as determined by DSC, the melting of the neat alkyl esters occurred at temperatures well above 5°C (see further discussion associated to Fig. 3B). Within this context, we assumed that the alkyl esters' crystal polymorph present at 5°C was the same that at -5°C. The X-ray diffractograms (WAXS and SAXS) for the neat SE and AE are shown in the Fig. 1SM to Fig. 5SM of the Supplementary Material. The *d* value determined in the SAXS region (Table 1) was associated with the length of the repetition structural unit formed by the alkyl ester molecules in the crystal. In both type of esters the *d* values were shorter than the thicknesses of a lamellar structure resulting from two stacked alkyl chain molecules and larger than a single molecule. Unfortunately, we could not find reports in the literature about the molecular organization of neat alkyl esters in the solid state. Within this context, we propose that the SAXS *d* value resulted of structural units formed by parallel interdigitated alkyl chain molecules, possible with an inclination angle. This organization would allow the stabilization of the structure along the parallel hydrocarbon chains through van der Waals forces and, allegedly through hydrogen bonds developed between the oxygen of the carbonyl group and an alpha hydrogen of the parallel alkyl ester molecule. Preliminary results obtained by our group through molecular mechanics simulations showed that, in addition to intermolecular dispersion forces, the formation of hydrogen bonds between parallel interdigitated alkyl ester molecules might occur between the parallel hydrocarbon chains. Within this framework, the length of the repetition unit determined by X-ray diffraction for the SE showed values of 44.64 Å, 52.02 Å, 62.80 Å, 71.83 Å, and 82.28 Å for the 14:14, 16:16, 18:18, 20:20, and 22:22, respectively; and for the AE of 67.28 Å, 67.28 Å, and 65.21 Å for 18:16, 18:20, and 18:22, respectively (Table 1). It was interesting to note that for the SE the length of the repetition unit showed a significant linear relationship with the number of carbons of the alkyl ester ($R^2 = 0.997$, $P < 0.001$). In contrast, for the AE the 18:16, 18:20, and

18:22 had a similar repetition unit length, this despite the increase in the carbon number from 34 (18:16) to 40 (18:22). This behavior was not observed by the 18:14 ester. The 18:14 was the only alkyl ester that showed two short-angle spacings at 43.49 Å and 52.34 Å, indicating that neat 18:14 crystallized in two different polymorphs. We also observed these two 18:14 polymorphs in the corresponding melting thermogram (results show later in Fig. 6SM panel B). Thus, the polymorphism might be associated with the different behavior of the 18:14 unit length when compared with the mean unit length's observed by 18:16, 18:20, and 18:22 (66.59 Å ± 1.19 Å). On the other hand, the *d* values showed by the alkyl esters in the WAXS region corresponded to higher order diffractions in the progression shown by a lamella packing arrangement. Thus, the diffractograms for the AE and for 20:20 and 22:22 showed the characteristic *d* values for an orthorhombic subcell with WAXS diffraction peaks at approximately 3.8 Å and 4.2 Å (Table 1). In contrast, 14:14, 16:16 and 18:18 did not show a diffraction pattern that supported their assignation to a particular subcell structure (Table 1). Nevertheless, similar to neat *n*-alkanes that crystallize in the monoclinic subcell structure, the major diffraction peak for these alkyl esters appeared at 4.2 Å. Thus, the neat 14:14, 16:16 and 18:18 were tentatively associated to a monoclinic subcell structure. We also observed that except 16:16, the relative intensity of the SE diffractograms was weaker in the SAXS region than in the WAXS region (Figs. 1SM to 3SM; Supplementary Material). This difference in the diffraction intensity was higher the longer the alkyl chains of the SE. These results showed that the molecular interactions within the lamellar planes (i.e., interplanar short spacings) of SE crystals occurred more frequently than those between the parallel interdigitated alkyl chain molecules. The parallel interdigitated chain molecules were aligned along the axis vertical to the interplanar plane (i.e., long spacings). The overall result was that, except 16:16, the neat SE crystals had a lower growth along the axis perpendicular to the lamellar plane in comparison with the interplanar growth. Consequently, we might expect that neat SE crystallized developing mainly plate-like crystals. In contrast, the AE diffractograms showed a lower diffraction signal in the WAXS region than in the

SAXS region (Figs. 4SM to Fig. 5SM; Supplementary Material). Therefore, the neat AE crystallized along the axis vertical to the interplanar plane, thus developing mainly acicular-like crystals. Unfortunately, PLM photographs of neat alkyl esters were very difficult to obtain. This, mainly because under the experimental conditions neat esters crystallized very fast overcrowding the field and making impossibly to distinguish crystals' shape and size. Within this context we decided to evaluate the crystal shape developed by the alkyl esters using concentrated vegetable oil solutions (60% wt/wt). We assumed that at this high concentration the effect of minor components or the triacylglycerides of the vegetable oil did not affect the crystallization habit of the alkyl esters of that occurring in the neat state. The PLM for the 60% solutions for some AE (i.e., 18:14 and 18:20) and SE (i.e., 16:16 and 20:20) are shown in Figs. 1 and 2. In the 60% ester solutions the 18:14 and 18:20 developed fibrillar crystals while the 16:16 and 20:20 formed plate crystals. These results showed that the symmetry or asymmetry of the alkyl ester had an effect in the crystal shape.

The crystallization and melting thermograms for the neat AE and SE are shown in Fig. 6SM (Supplementary Material), and the T_{Cr}, T_M, ΔH_{Cr}, and ΔH_M behavior as a function of the ester's carbon number are shown in Figs. 3 and 4. Using low molecular weight gelators in the neat state and in vegetable oil solution, our group established that the gelator's molecular structure is associated with the onset of their molecular self-assembly (i.e., T_{Cr}) (Toro-Vazquez et al., 2013). In the same way we established that the gelator's solubility temperature in the vegetable oil is indirectly associated with T_{Cr}, while T_M and the heats of melting (ΔH_M) and crystallization (ΔH_{Cr}) are associated with the energies of the molecular interactions that stabilize the crystal structure in the neat state and in the oleogel (Toro-Vazquez et al., 2013)**.** Within this context, independent of the type of alkyl ester (i.e., SE or AE), T_{Cr} and T_M of the neat alkyl esters had a direct linear relationship with the carbon number ($P < 0.005$; Fig. 3). The linear equations reported in Figs. 3A and 3B indicated that the increase of just one carbon in the alkyl chain of SE and AE resulted in a T_{Cr} and T_M increment of about 2°C. In other words, independent of the type of ester, the longer the ester hydrocarbon chain the higher the

onset temperature for its molecular self-assembly (i.e., higher T_{Cr}). In the same way, the longer the alkyl ester the higher the temperature to achieve the complete breakup of the non-covalent interactions stabilizing the alkyl ester crystals (i.e., higher T_M). Similar results for T_M have been reported for neat *n*-alkanes with even and odd carbon number between 7 and 32 (Boese et al., 1999; McGann and Lacks, 1999). These results showed that T_{Cr} and T_M of the alkyl esters in the neat state depend essentially on the carbon number. Consequently, the longer the alkyl esters chain the higher the onset temperature for the molecular self-assembly (i.e., T_{Cr}) and more significant the van der Waals forces became for molecular self-assembly and crystal structure stabilization (i.e., higher T_M). The results shown in Fig. 3 showed that the symmetry or asymmetry of the alkyl esters studied did not affect the T_{Cr} and T_M behavior as a function of the carbon number.

On the other hand, in comparison with T_{Cr} and T_M the ΔH_{Cr} and ΔH_M of the neat alkyl esters showed a different behavior as a function of the carbon number (Fig. 4). Thus, ΔH_{Cr} and ΔH_M for the SE observed a quadratic increase as a function of the carbon number ($R^2 > 0.89$; $P < 0.001$). In contrast, for the AE the 18:16, 18:20, and 18:22 showed statistically the same ΔH_{Cr} and ΔH_M with mean values of 141.5 kJ/mol (± 7.4 kJ/mol) and 138.0 kJ/mol (± 7.7 kJ/mol), respectively. However, of all AE studied 18:14 showed the lower ΔH_{Cr} (109.7 ± 4.2 kJ/mol) and ΔH_M (107.2 ± 6.3 kJ/mol) values, a behavior surely associated with its polymorphic behavior as established previously by X-ray analysis (Fig 4SM panel A; Supportive Information). The 18:14 polymorphic behavior was also observed in the corresponding melting thermogram as one minor endotherm around 38°C followed by a major endotherm around 49°C (Fig. 6SM panel B). The ΔH_M plotted for 18:14 in Fig. 4B was just for the major exotherm. Thus, the lower ΔH_{Cr}, ΔH_M, and shorter length of the repetition unit of 18:14 (Table 1; Fig. 4) were the result of its polymorphism. Thus, ΔH_{Cr} and ΔH_M for the AE followed a similar trend as the repetition unit length previously discussed, i.e., 18:16, 18:20, and 18:22 had the same repetition unit length (66.59 Å ± 1.19 Å) while 18:14 showed two short-angle spacings at 43.49 Å and 52.34 Å. These results along with the X-ray diffractograms

(Figs. 1SM to 5SM) and PLM (Figs. 1 and 2) observations showed that the symmetry or asymmetry of the ester molecules had a significant effect in the crystallization of neat esters. We also observed an additional difference in the crystallization behavior between SE and AE. It is well established that supercooling, i.e., the difference between the melting and the crystallization temperature of a compound, provides the thermodynamic drive for the molecular self-assembly of gelator molecules. Thus, from the corresponding thermograms of each ester we calculated the difference between the temperature at the end of melting ($T_{M\text{-}End}$) and the onset temperature for crystallization ($T_{Cr\text{-}O}$). Within this context, the difference $T_{M\text{-}End}$ - $T_{Cr\text{-}O}$ for the ester solutions was considered as a relative measurement of the supercooling required to achieve the alkyl ester crystallization. The Figure 7SM showed that the relative supercooling required to achieve the molecular self-assembly of AE increased linearly ($R^2 = 0.78$; $P < 0.10$) as a function of the carbon number while for SE decreased ($R^2 = 0.80$; $P < 0.05$). Thus, as the carbon number increased the molecular self-assembly of the AE was harder to achieve than for the SE (Fig. 7SM). However, the energy required for melting (ΔH_M) of the orthorhombic crystals developed by 18:16, 18:20, and 18:22 was statistically the same (Fig. 4B). This, in spite of the increase in the carbon number for these AE. In contrast, the energy required for melting of the SE crystals increased quadratically as a function of the carbon number (Fig. 4B), achieving a plateau above 40 carbons (20:20). Above a carbon number of 40 the SE crystallized in the orthorhombic phase while below 40 carbons (i.e., 14:14, 16:16 and 18:18) as monoclinic (Table 1). Based on the supercooling behavior show in Fig. 7SM, the crystal shape and polymorph developed by alkyl esters would depend on their symmetry or asymmetry and in their length.

3.2. BEHAVIOR OF THE ASYMMETRIC AND SYMMETRIC ESTERS IN VEGETABLE OIL SOLUTION

We used the Hildebrand equation (Eq. 1) to fit the corresponding thermal parameters obtained with the 0.5% to 5% (wt/wt) ester oil solutions. With the cooling program used

14:14 solutions below 3% did not achieve full crystallization. Therefore, to have enough experimental data just for the 14:14 ester we included the 6% ester concentration. The results showed that for all ester solutions the Hildebrand equation (Eq. 2; section 2.3.2) fitted the change of T_S (i.e., melting temperature of the alkyl ester in the oil solution, T_M) as a function of the ester molar fraction with a determination coefficient (r^2) above 0.90 ($P < 0.01$). The Hildebrand equation parameters for the AE and SE solutions in vegetable oil and corresponding statistical significance of the linear regression are reported in Table 1SM of the Supplementary Material. These results showed that within the concentration interval used for the AE and SE solutions (Table 1SM), the alkyl esters behave as ideal solutes in the vegetable oil, i.e., the melting temperature of the AE and SE in the vegetable oil was a direct function of the alkyl ester concentration. Within the previous context we used the corresponding Hildebrand equation (Table 1SM of the Supplementary Material) to estimate the ΔH_M and T_M values for the neat AE and SE assuming an *X* value of 1 (i.e., ΔH_M and T_M were the estimated values for the neat esters). Subsequently, we determined the percentage of absolute error when these values where used as predictors of the corresponding experimental ΔH_M and T_M values. The results showed that, independent of the type of ester, the predicted T_M had an absolute error lower than 9%. In contrast, the predicted ΔH_M for the neat SE had an absolute error between 15% and 51%. On the other hand, except the equation for 18:14 that provided an absolute error of 18%, the predicted ΔH_M for the neat AE had an absolute error lower than 9%. Evidently, the SE developed a different crystal organization (i.e., polymorph) crystallizing from the vegetable oil solution than from the melt, and from there the large differences observed between the predicted and the experimental ΔH_M value. In contrast, except 18:14, the AE in vegetable oil solutions and from the melt crystallized developing the same polymorph (i.e., orthorhombic; Table 1). As already discussed, 18:14 was the only ester that showed the development of two polymorphs, a phenomenon probably associated to the low predictive capacity of the estimated ΔH_M value. Unfortunately, we could not corroborate these conclusions with experimental measurements since at the ester concentration used in the

vegetable oil (i.e., lower than 6%), the X-ray signal of our equipment was low and did not provide reliable diffractograms.

3.3. RELATIONSHIP BETWEEN THE RHEOLOGY AND MICROSTRUCTURE OF THE ASYMMETRIC AND SYMMETRIC ESTERS OLEOGELS

The development of an organogel requires the formation of a self-supporting structure by the gelator's molecules that physically trap the organic solvent. The minimal gelling concentration of a gelator (i.e., vegetable wax, alkyl ester), also known as the critical gelling concentration, is associated to the minimal mass of crystals that develops the self-supporting structure in a giving solvent (i.e., vegetable oil). This gelling parameter is function of the gelator solubility in the solvent as affected by time-temperature conditions (i.e., gel setting temperature, cooling rate) (Toro-Vazquez and Pérez-Martínez, 2018). Thus, the minimal gelator concentration for vegetable waxes with significant concentration of alkyl esters (e.g., carnauba wax, rice hull wax, safflower wax) has been reported between 1% and 5% by different authors (Dassanayake et al., 2009; Blake et al., 2014; Patel et al., 2015). However, there are not minimal or critical gelator concentration data reported in the literature for neat alkyl esters in vegetable oil or any other solvent. Unfortunately, because limited availability of pure esters, we could not experimentally determine their minimal gelator concentration. Working with *n*-alkanes with 24, 28, 32 and 36 carbons and several organic solvents, Abdallah and Weiss (2000) reported critical gelator concentrations >5.1%, >2.1%, 2.3% and 1.3%, respectively. In the same way, using silicon oil, mineral oil and decane as solvents Pal et al., (2013) reported critical gelator concentrations between 0.6% and 3.8% for a series of positional isomers of keto octadecanoic acid (i.e., carboxylic acids with a carbonyl group inserted in different positions). However, none of these studies used vegetable oil as solvent. Thus, we established a 3% (wt/wt) ester concentration to compare the thermo-mechanical properties of AE and SE oleogels with and without MSG. As already mentioned, the monoglycerides are minor native components

present in vegetable oils. However, once intentionally added to the vegetable oil to develop emulsions or organogelled emulsions, their amphiphilic character and capability of developing hydrogen bonds might favor or hinder the self-assembly of the alkyl esters.

The *G'*, measured at -5°C, as a function of the carbon number for the 3% AE and SE oleogels with 0%, 0.5%, and 1% of MSG are shown in Fig. 5. As established by DSC, at -5°C we assured the complete crystallization of the alkyl ester and MSG present in the vegetable oil solutions. The PLM photographs for the corresponding SE oleogels with 0%, 0.5% and 1% MSG are shown in Figs. 6 to 8 and for the AE oleogels in Figs. 9 to 11. Independent of the MSG concentration we achieved the highest oleogel's elasticity in the AE and SE oleogels developed with the 32 carbons esters (i.e., 16:16 and 18:14; $P < 0.05$) (Fig. 5). Above 32 carbons, independent of the MSG concentration, the elasticity of the SE oleogels showed a decreasing trend as the carbon number increased (Fig. 5). The AE oleogels with 0% MSG also showed a similar *G'* decreasing behavior (Fig. 5A). Nevertheless, in all cases the AE oleogels had higher *G'* than the SE oleogels, particularly in the presence of MSG (Figs. 5B and 5C). Hwang et al., (2012) reported that wax esters with longer alkyl chains esters required lower quantity to achieve gelation that waxes with shorter alkyl chains. The results in Fig. 5A showed that the esters' gelation capability in vegetable oils depends not only on the alkyl chain length, but also on the symmetry or asymmetry of the alkyl chains respect to the ester bond. However, it is important to note that, in contrast with the study of Hwang et al., (2012) that used native waxes (i.e., mixtures of wax esters) containing other additional minor components, the present study used pure saturated alkyl esters. The PLM for the oleogels with 0% MSG showed that, overall, the AE crystals were larger (Fig. 9) than those developed by the SE (Fig. 6). Additionally, the AE crystallized in acicular shaped crystals while the SE crystallized mainly as plate-like shaped crystals. This was evident when comparing the PLM of oleogels developed by esters with the same carbon number, i.e., 18:14 and 16:16, and particularly the 18:22 and 20:20 esters (Figs. 6 and 9). These observations agreed with the

microestructure developed by the alkyl esters in the 60% ester solutions previously discussed (Figs. 1 and 2). For the SE oleogels with 0% MSG the crystals' size increased from the ester with 28 carbons (i.e., 14:14) up to 40 carbons ester (i.e., 20:20). The increase in crystal size resulted in lower extent of crystal-crystal interaction, and therefore in the crystal network's strength. The overall effect was a reduction in the elasticity of the SE oleogels as the carbon number increased from 32 (16:16) up to 40 (20:20) (Figs. 5A and 6). In contrast, the 22:22 oleogel was structured by smaller crystals (Fig. 6) that resulted in an increase in *G'*. However, the increase in *G'* was not statistically different from the elasticity provided by the 20:20 oleogels (Figs. 5A and 6). The AE oleogels with 0% MSG also showed an increase in crystal size as the carbon number increased, a behavior associated with the decrease in the oleogels' elasticity (Figs. 5A and 9). The results showed in Fig. 5A and Figs. 6 and 9 indicated that the AE oleogels structured by large acicular crystals (18:14, 18:16, 18:20, and 18:22, Fig. 9) resulted in gels with higher *G'* when compared with the SE oleogels structured by smaller plate-like crystals (16:16, 18:18, 20:20, and 22:22, Fig. 6). Thus, crystal shape in addition to size determined the oleogels rheology. These results agreed with those obtained previously with low molecular weight gelators in the neat state and in oleogels (Toro-Vazquez et al., 2013). In particular, the 18:22 oleogel was structured by bundles of large fibers (Fig. 9) that would increase the crystal-crystal interaction resulting in higher oleogel elasticity than the one achieved by the 20:20 oleogel (Fig. 5A, Fig. 6). It is important to note that cooling thermograms of the vegetable oil showed that its crystallization onset (i.e., development of a solid phase) occurred at between -15°C and -20°C. Additionally, rheological measurements of the vegetable oil under the time-temperature conditions to develop and measure the AE and SE oleogels, showed that *G''* was always greater of *G'*. These results showed that vegetable oil remained liquid at -5°C and therefore its contribution to the oleogels' elasticity was negligible.

Regarding the effect of MSG we noted that the addition of MSG increased the oleogels' elasticity independent of the type of ester and the ester carbon number (Fig. 5).

However, the MSG effect was higher in the AE oleogels than in the SE oleogels (Figs. 5B and 5C). In particular, the addition of just 0.5% of MSG limited the decrease in *G'* observed in the oleogels without MSG as the carbon number increased (Fig. 5). The addition of MSG had a dramatic effect in the ester's crystal size and shape (Figs. 7 and 8 for SE; Figs. 10 and 11 for the AE). This effect was particularly evident in the AE oleogels (compare the photographs of Fig. 9 with those in Figs. 10 and 11). Thus, in comparison with the microstructure of the AE oleogels with 0% MSG (Fig. 9), the addition of just 0.5% MSG to AE oleogels modified the crystal shape and, particularly, decreased the crystal size (Fig. 10). However, based on the microphotographs of the oleogels we considered that higher MSG concentrations (i.e., 1% MSG) had no additional effect in the crystal shape and size of the AE (Fig. 11). It is important to note that, in comparison with the oleogels with 0% MSG, the addition of MSG ought to result in approximately 0.5% or 1% increase in the oleogels' solid content. Rheological measurements of 0.5% and 1% MSG vegetable oil solutions at -5°C provided *G'* values of just around 40 Pa or lower, i.e., the solid phase developed by the MSG was not sufficient to form an oleogel. Nevertheless, the increase in the crystal mass (i.e., solid content) and decrease in the crystal size associated with the addition of MSG would result in higher crystal-crystal interaction, and subsequently in higher oleogels' elasticity, particularly in the AE with 38 and 40 carbons (Fig. 5).

We did a more detailed rheological analysis of the oleogels by plotting, for the SE and AE oleogels at the different MSG concentrations, the phase angle (δ) as a function of ω (Figs. 12 and 13). The δ parameter, defined as $\tan^{-1}(G''/G')$, is used to evaluate in a sensitive way the viscoelastic changes occurring in complex systems. Thus, in pure viscous systems, like the vegetable oil, δ = 90° since *G''* completely dominates *G'*. In contrast, δ = 0° in fully structured systems with ideal elastic behavior since *G'* completely dominates *G''*. When the viscous and elastic behavior are exactly balanced *G'* = *G''* and, therefore, δ = 45° (Mezger, 2014). Consequently, in gelled systems (i.e., oleogels) where *G'* > *G''* the δ values would be lower than 45° and the smaller the δ value the larger the gel's elasticity. The use of δ sweeps as a function of ω was

particularly useful because allows the study of viscoelastic changes occurring as a function of a timescale in complex systems like crystallization of triglycerides or phosphatidylcholine in vegetable or mineral oil (Martínez-Ávila et al., 2019; Toro-Vazquez et al., 2005). Within this context, in solid-like materials δ would have values lower than 45° with a rheological behavior nearly independent of δ (i.e., true gels). In contrast, the more δ behaves ω dependent showing values above 45° the more fluid like is the material (i.e., a sol or a gel-like material). Thus, except the 16:16 oleogel, the ω sweeps of the SE oleogels with 0% MSG showed δ values above 20°. In particular, the 14:14 and 18:18 oleogels with 0% MSG observed a frequency independent rheological behavior at a ω < 15 Hz with δ values between 30° and 40°. However, at higher ω the δ values increased up to values between 75° and 80° (Fig. 12A). In contrast, below 1.5 Hz the 20:20 oleogel with 0% MSG showed δ values that varied between 20° and 50°, while the 22:22 oleogel had δ values between 20° and 35°. Thus, below 1.5 Hz the 20:20 and 22:22 oleogels with 0% MSG showed frequency dependent rheological behavior that further continued at higher ω until δ achieved values around 50° to 55°. These results showed that the 14:14, 18:18, 20:20 and the 22:22 oleogels with 0% MSG were weak gels that would go through phase separation during storage. In fact these oleogels showed some visual phase some separation after about four to six weeks of storage at -5°C. The exception to this behavior was the 16:16 oleogel with 0% MSG. This oleogel showed essentially a frequency independent rheological behavior in most of the ω interval, providing δ values around 16° (Fig. 12A). Thus, the 16:16 oleogels with 0% MSG showed the rheological behavior of a true gel. However, the 16:16 oleogels' rheological behavior could not be explained considering just the oleogels' microstructure (Fig. 6). In contrast, the AE oleogels with 0% MSG had δ values well below 35° showing essentially a frequency independent rheological behavior. At ω higher than 0.3 Hz the AE oleogels with 0% MSG had a tendency of achieving lower δ values (i.e., higher elasticity) as the carbon number decreased from 18:22 (δ ≈ 20° to 29°) to 18:14 (δ ≈ 6° to 10°) (Fig. 13A). Thus, in contrast with the SE oleogels with 0% MSG all the AE oleogels with 0% MSG showed the rheological

behavior of a true gel. Within this context it is important to point out that for the same carbon number, the AE oleogels (i.e., 18:14, 18:22) had significantly lower δ values (i.e., higher elasticity) than the corresponding SE oleogels (i.e., 16:16, 20:20) (Figs. 12A and 13A). The difference in rheological behavior between the SE and AE oleogels with 0% MSG was explained considering the oleogels microstructure previously discussed (Figs. 6 and 9) and its effect in the crystal-crystal interaction and therefore in the oleogels elasticity. Nevertheless, as previously indicated, the 16:16 oleogel with 0% MSG was the only SE that showed a ω independent rheological behavior as the AE oleogels (Figs. 12A and 13A). The 16:16 oleogel had a microstructure closer to that developed by the AE oleogels (Figs. 6 and 9), and possible this was the reason the 16:16 oleogel showed similar ω independent rheological behavior as the AE oleogels. Within this context, as previously noted, the neat 16:16 was the only SE that showed a similar X-ray diffraction pattern to neat AE. Thus, like the neat AE the X-ray diffraction for 16:16 showed a lower diffraction signal in the WAXS region than in the SAXS region. Unfortunately, we could not find the reasons why the particular crystallization and rheological behavior of the 16:16 ester in the neat state and the oleogel. We did not consider that the rheological behavior showed by the AE and SE oleogels with 0% MSG was associated with differences in the oleogels' solid content. As already discussed, at the gel setting temperature used for rheological measurements (-5°C), we assured the complete crystallization of all the alkyl esters (i.e., 3%). Thus, cooling thermograms of the 3% alkyl esters solutions in the vegetable oil showed that the corresponding crystallization exotherm ended at a temperature well above the gel setting temperature (from -1.7°C for the 14:14 oleogel up to 37.2°C for the 22:22 oleogel). Unfortunately, due to the limited amount of pure esters available we could not determine the oleogels' solid content. Therefore, the rheological behavior of the SE and AE oleogels with 0% MSG was mainly associated with the microestructural organization of the alkyl esters in the oleogels (Figs. 6 and 9).

On the other hand, independent of the type of ester, the addition of 0.5% MSG and particularly 1% MSG resulted in gels that provided lower δ values (Figs. 12B, 12C, 13B

and 13C) and, therefore, better structured than the oleogels with 0% MSG (Figs. 12A and 13A). Except the δ behavior observed by the 18:20 and 20:20 oleogels with 1% MSG at ω lower than 0.30 Hz (Figs. 12C and 13C), and the 14:14 oleogel with 0.5% MSG at ω above 50 Hz (Fig. 12B), all the AE and SE oleogels with 0.5% or 1% MSG showed δ values lower than 30° with ω independent rheological behavior (Figs. 12B, 12C, 13B and 13C). In contrast with the oleogels with 0% MSG, we considered that the rheological behaviors of the SE and AE oleogels with 0.5% and 1% MSG were associated with the microestructural organization of the oleogels previously discussed (Figs. 7 and 8 for the SE, and Figs. 10 and 11 for the AE), but also with the higher solid content associated with the MSG crystallization. Other studies had shown that the presence of minor components of vegetable oils (i.e., tripalmitin) have a profound effect in the gelation capability and the molecular self-assembly mechanism of the hentriacontane (i.e., *n*-alkane with 31 carbons) present in candelilla wax (Chopin-Doroteo et al., 2011; Morales-Rueda et al., 2009). As previously discussed, we observed that a small amount of MSG modified the crystal habit of neat alkyl esters (Figs. 7 and 8), developing oleogels with higher elasticity than the ester oleogels (Figs. 5B and 5C). As examples, the Figures 8SM and 9SM of the Supplementary Material show cooling and heating thermograms for a symmetrical (i.e., 18:18) and asymmetrical (i.e., 18:16) oleogels with 0.5% and 1% MSG, in comparison with the corresponding independent systems, i.e., the 3% alkyl ester oleogel and the corresponding 0.5% and 1% MSG solution in the vegetable oil. The photographs for these oleogels obtained at -5°C through PLM are included in the Figs. 8SM and 9SM. We noted than the crystallization and further melting of the MSG in the corresponding 0.5% and 1% solutions were modified when occurred in the alkyl ester-MSG oleogels. Thus, during cooling and further melting of the independent systems the 3% alkyl esters, the 0.5% and 1% MSG showed exotherms and endotherms of different shapes, T_{Cr} and T_M. However, during cooling of the alkyl ester-0.5% MSG and alkyl ester-1% MSG systems both gelators crystallized showing just one exotherm. Upon heating the oleogels melted showing just one exotherm that, except the 18:18 and 18:22 alkyl

esters, had a T_M statistically equal to the T_M of the corresponding 3% alkyl ester-0% MSG oleogel (see Table 2SM of the Supplementary Material). Within this context, the DSC results of alkyl esters-MSG oleogels suggested that the alkyl ester and the MSG crystallized as one entity, i.e., a co-crystal. It is important to point out that during melting of some of the alkyl ester-MSG oleogels we observed a small shoulder of the major melting endotherm (see arrow in the heating thermogram for the 3%18:18-1% MSG oleogel, Fig. 8SM panel D). We associated this thermal behavior with the melting of MSG that apparently did not co-crystallize with the alkyl ester during cooling. This might be the reason why the 18:18 and 18:22 alkyl esters oleogels with 0.5% and 1% MSG showed an endotherm with a higher T_M than the corresponding alkyl esters oleogels with 0% MSG ($P < 0.05$; Table 2SM of the Supplementary Material).

The tentative alkyl esters-MSG co-crystals might develop through van deer Walls forces established between the hydrocarbon chain of the stearic acid esterified to the MSG and the alkyl chains of the AE or SE. This would result in a modification of the original ester self-assembly and, subsequently, in the crystal size and shape. The calorimetry results also showed that in alkyl ester-MSG oleogels, particularly developed with 1% MSG, part of the MSG did not interact with the ester molecules and crystallized independently of the co-crystals. These MSG crystals might act as active fillers of the major microstructure developed by the alkyl ester-MSG co-crystals. The overall effect was that the alkyl ester-MSG oleogels had higher *G'* with a δ frequency independent rheological behavior in comparison with the alkyl ester oleogels with 0% (Figs. 5, 12 and 13).

The results of this study showed that alkyl ester composition and structure (i.e., symmetry or asymmetry) greatly influences its molecular self-assembly, with the consequent effect in the oleogel's thermo-mechanical properties. Additionally, MSG commonly used in the development of organogelled emulsions (Toro-Vazquez et al., 2013), affected the alkyl ester crystallization resulting in oleogels with higher elastic properties with frequency independent rheological behavior. The rheological properties of the alkyl esters-MSG oleogels were associated with the development of co-crystals

between the ester and the monoglyceride. Additionally, part of the MSG that did not interact with the ester molecules and crystallized independently, acted as an active filler of the three-dimensional microstructure formed by the co-crystals. The relevance of these results resides in the major role that alkyl esters play in establishing the functional properties of vegetable wax's oleogels used in food systems and cosmetics. Ongoing studies using molecular mechanics modeling are underway to establish the mechanism for AE and SE self-assembly with and without MSG.

4. ACKNOWLEDGMENTS

The present research was supported by Consejo Nacional de Ciencia y Tecnología (CONACYT) through the grant CB-280981-2018. G. Avendaño-Vásquez greatly appreciates the scholarship provided by CONACYT to conclude her Ph.D. program. The technical support from Marisol Davila Martínez is greatly appreciated

5. CONFLICT OF INTEREST

The authors declare that they have no conflicts of interest.

6. AUTHOR CONTRIBUTIONS STATEMENT

AV is currently a Ph. D. student and these results are part of her thesis research. AV was closely involved in the DSC, rheological measurements and implementing the microscopy technique to evaluate the crystallization of the esters in the neat state and in the oleogels; DG and CAME were mainly involved in doing the X-ray analysis and their diffractograms interpretation within the context of the symmetrical and asymmetrical ester molecular self-assembly; CAMA and TV established the experimental conditions used in this study, integrated and analyzed all data. DG, CAMA and TV obtained and analyze the data associated with the Hildebrand equation

applied to the crystallization and melting behavior of the ester in vegetable oil solutions. TV was the project and research group leader, also acting as AV's thesis advisor.

7. CONTRIBUTION TO THE FIELD STATEMENT

The food industry faces the need to develop *trans*-free food products low in saturated fatty acids, due to their negative effect on the cardiovascular health. Several studies have shown that organogelation is a useful and novel alternative to structure vegetable oils (i.e., oleogels) without the use of *trans* and/or saturated fats. Commercial vegetable waxes have a significant content of long chain saturated alkyl esters. Consequently, alkyl esters play an important role in determining the functional properties of vegetable waxes. Nevertheless, there is limited information about the physical properties of alkyl esters either in pure state or in oleogels. We studied the relationship between the physical properties of typical alkyl esters (saturated with symmetric or asymmetric structure) present in vegetable waxes and the microstructure developed by the alkyl ester in the neat state and in oleogels. Additionally, we studied the effect of monoglycerides, a minor component present in vegetable oils, in the development of alkyl ester oleogels. We established that ester composition and structure (i.e., symmetry or asymmetry) greatly influences their mechanism of crystallization, determining relevant physical properties associated with the oleogel's texture (i.e., elasticity). The oleogels' elasticity was significantly improved by the presence of small quantities of monoglycerides, mainly because the monoglycerides developed co-crystals with the alkyl esters. These results showed the major role that alkyl esters play in establishing the functional properties of vegetable wax's oleogels.

8. REFERENCES

Abdallah, D. J., and Weiss, R. G. (2000). n-Alkanes gel n-alkanes (and many other organic liquids). Langmuir, 16(2), 352–355. https://doi.org/10.1021/la990795r

Abraham, S., Lan, Y., Lam, R. S. H., Grahame, D. A. S., Kim, J. J. H., Weiss, R. G., and Rogers, M. A. (2012). Influence of positional isomers on the macroscale and nanoscale architectures of aggregates of racemic hydroxyoctadecanoic acids in their molecular gel, dispersion, and solid states. Langmuir, 28(11), 4955–4964. https://doi.org/10.1021/la204412t

Alvarez-Mitre, F. M., Morales-Rueda, J. A., Dibildox-Alvarado, E., Charó-Alonso, M. A., and Toro-Vazquez, J. F. (2012). Shearing as a variable to engineer the rheology of candelilla wax organogels. Food Research International, 49(1), 580–587. https://doi.org/10.1016/j.foodres.2012.08.025

Blake, A. I., Co, E., and Marangoni, A. G. (2014). Structure and physical properties of plant wax crystal networks and their relationship to oil binding capacity. JAOCS, Journal of the American Oil Chemists' Society, 91(6), 885–903. https://doi.org/10.1007/s11746-014-2435-0

Blake, A. I., Toro-Vazquez, J. F., and Hwang, H.-S. (2018). Wax Oleogels, in Edible Oleogels. Structure and Health Implications,ed. Alejandro G. Marangoni, Nissim Garti. (San Diego, USA: AOCS Press),133-171. https://doi.org/10.1016/b978-0-12-814270-7.00006-x

Boese, R., Weiss, H. C., and Bläser, D. (1999). The melting point alternation in the short-chain n-alkanes: Single-crystal X-ray analyses of propane at 30 K and of n-butane to n-nonane at 90 K. Angewandte Chemie - International Edition, 38(7), 988–992. https://doi.org/10.1002/(SICI)1521-3773(19990401)38:7<988::AID-ANIE988>3.0.CO;2-0

Bot, A., and Agterof, W. G. M. (2006). Structuring of edible oils by mixtures of γ-oryzanol with β-sitosterol or related phytosterols. JAOCS, Journal of the American Oil Chemists' Society, 83(6), 513–521. https://doi.org/10.1007/s11746-006-1234-7

Bot, A., Den Adel, R., and Roijers, E. C. (2008). Fibrils of γ-oryzanol + β-sitosterol in edible oil organogels. JAOCS, Journal of the American Oil Chemists' Society, 85(12), 1127–1134. https://doi.org/10.1007/s11746-008-1298-7

Bot, A., den Adel, R., Roijers, E. C., and Regkos, C. (2009). Effect of sterol type on structure of tubules in sterol + γ-oryzanol-based organogels. Food Biophysics, 4(4), 266–272. https://doi.org/10.1007/s11483-009-9124-9

Busson-Breysse, J., Farines, M., and Soulier, J. (1994). Jojoba wax: Its esters and some of its minor components. Journal of the American Oil Chemists' Society, 71(9), 999–1002. https://doi.org/10.1007/BF02542268

Chen, C. H., Damme, I. V., and Terentjev, E. M. (2009). Phase behavior of C18 monoglyceride in hydrophobic solutions. 432–439. https://doi.org/10.1039/b813216j

Chopin-Doroteo M., Morales-Rueda J. A., Dibildox-Alvarado E., Charó-Alonso M. A., de la Peña-Gil A., and Jorge F. Toro-Vazquez.(2011). "The Effect of Shearing in the Thermo-Mechanical Properties of Candelilla Wax and Candelilla Wax-Tripalmitin Organogels."Food Biophysics 6 (3): 359–76. https://doi.org/10.1007/s11483-011-9212-5.

Co, E., and Marangoni, A. G. (2012). Organogels: An alternative edible oil-structuring method. JAOCS, Journal of the American Oil Chemists' Society, 89(5), 749–780. https://doi.org/10.1007/s11746-012-2049-3

Co, E., and Marangoni, A. G. (2013). The formation of a 12-hydroxystearic acid/vegetable oil organogel under shear and thermal fields. JAOCS, Journal of the American Oil Chemists' Society, 90(4), 529–544. https://doi.org/10.1007/s11746-012-2196-6

Cosmetic Lab, S. C.(2016) 9 MOST IMPORTANT NATURAL WAXES FOR COSMETICS (PART II). https://skinchakra.eu/blog/archives/411-9-most-important-natural-waxes-for-cosmetics-Part-II.html [Accessed February 20, 2019].

Dassanayake, L. S. K., Kodali, D. R., and Ueno, S. (2011). Formation of oleogels based on edible lipid materials. Current Opinion in Colloid and Interface Science, 16(5), 432–439. https://doi.org/10.1016/j.cocis.2011.05.005

Dassanayake, L. S. K., Kodali, D. R., Ueno, S., and Sato, K. (2009). Physical properties of rice bran wax in bulk and organogels. JAOCS, Journal of the American Oil Chemists' Society, 86(12), 1163–1173. https://doi.org/10.1007/s11746-009-1464-6

Doan, C. D., To, C. M., De Vrieze, M., Lynen, F., Danthine, S., Brown, A., Dewettinck, K., and Patel, A. R. (2017). Chemical profiling of the major components in natural waxes to elucidate their role in liquid oil structuring. Food Chemistry, 214, 717–725. https://doi.org/10.1016/j.foodchem.2016.07.123

Ferrari, V., and Mondet, J.,inventor; L´Oreal S. A., assignee. Care and/or Make-Up Cosmetic Composition Structured with Silicone Polymers and Organogelling Agents, in Rigid Form. International WO/2003/105788 (2003). https://patentscope.wipo.int/search/en/detail.jsf?docId=WO2003105788

Fórmula Botánica. (2019) 6 Vegan Waxes for Organic Cosmetic Formulations. https://formulabotanica.com/6-vegan-waxes/[Accessed February 20, 2019].

Gandolfo, F. G., Bot, A., and Flöter, E. (2004). Structuring of Edible Oils by Long-Chain FA, Fatty Alcohols, and Their Mixtures. JAOCS, Journal of the American Oil Chemists' Society, 81(1), 1–6. https://doi.org/10.1007/s11746-004-0851-5

Ghamdi, A. K. Al, Elkholy, T. A., Abuhelal, S., Alabbadi, H., Qahwaji, D., Sobhy, H., Khalefah, N., and Abu Hilal, M. (2017). Study of Jojoba (Simmondsia chinensis) Oil by Gas Chromatography. Natural Products Chemistry & Research, 05(06). https://doi.org/10.4172/2329-6836.1000283

Gunstone, F D. (2002). Vegetable Oils in Food Technology: Composition, Properties, and Uses. Copenhagen, Denmark: Blackwell Publishing Ltd

Han, L., Li, L., Li, B., Zhao, L., Liu, G. Q., Liu, X., and Wang, X. (2014). Structure and physical properties of organogels developed by sitosterol and lecithin with sunflower oil. JAOCS, Journal of the American Oil Chemists' Society, 91(10), 1783–1792. https://doi.org/10.1007/s11746-014-2526-y

Hildebrand, J. H., and Robert-Lane S., (1950) The solubility of nonelectrolytes (3rd ed). New York, N.Y. : Reinhold.

Hwang, H. S., Sanghoon K., Mukti S., Jill K. W.M., and Liu S. X. (2012). “Organogel Formation of Soybean Oil with Waxes.” JAOCS, Journal of the American Oil Chemists’ Society 89 (4): 639–47. https://doi.org/10.1007/s11746-011-1953-2.

Hwang, H. S., Singh, M., Winkler-Moser, J. K., Bakota, E. L., and Liu, S. X. (2014). Preparation of margarines from organogels of sunflower wax and vegetable oils. Journal of Food Science, 79(10), C1926–C1932. https://doi.org/10.1111/1750-3841.12596

Lam, R. S. H., and Rogers, M. A. (2011). Activation energy of crystallization for trihydroxystearin, stearic acid, and 12-hydroxystearic acid under nonisothermal cooling conditions. Crystal Growth and Design, 11(8), 3593–3599. https://doi.org/10.1021/cg200553t

López-Martínez, A., Morales-Rueda, J. A., Dibildox-Alvarado, E., Charó-Alonso, M. A., Marangoni, A. G., and Toro-Vazquez, J. F. (2014). Comparing the crystallization and rheological behavior of organogels developed by pure and commercial monoglycerides in vegetable oil. Food Research International, 64, 946–957. https://doi.org/10.1016/j.foodres.2014.08.029

Marangoni, A. G., and Garti, N. (2011). Edible Oleogels structure and health implications. Indiana, IL: AOCS Press https://doi.org/10.1016/B978-0-9830791-1-8.50007-3

Marangoni, A.G., and Garti, N. (2018). Edible Oleogels Structure and Health Implications. Second edition. Indiana, IL: AOCS Press. https://doi.org/https://doi.org/10.1016/B978-0-12-814270-7.01001-7

Martínez-Ávila, M., De la Peña-Gil, A., Álvarez-Mitre, F. M., Charó-Alonso, M. A., and Toro-Vazquez, J. F. (2019). Self-Assembly of Saturated and Unsaturated Phosphatidylcholine in Mineral and Vegetable Oils. JAOCS, Journal of the American Oil Chemists’ Society, 96(3), 273–289. https://doi.org/10.1002/aocs.12188

McGann, M. R., and Lacks, D. J. (1999). Chain length effects on the thermodynamic properties of n-alkane crystals. Journal of Physical Chemistry B, 103(14), 2796–2802. https://doi.org/10.1021/jp983932m

Mezger, Thomas G. (2014). The Rheology Handbook: For users of rotational and oscillatory rheometers (4th ed). Hanover, Germany: Vincentz Network. https://doi.org/10.1108/prt.2009.12938eac.006.

Morales-Rueda, J. A., Dibildox-Alvarado, E., Charó-Alonso, M. A., Weiss, R. G., and Toro-Vazquez, J. F. (2009). Thermo-mechanical properties of candelilla wax and dotriacontane organogels in safflower oil. European Journal of Lipid Science and Technology, 111(2), 207–215. https://doi.org/10.1002/ejlt.200810174

Morales, M., Gallardo, V., Clarés, B., García, M., and Ruiz, M. (2010). Study and description of hydrogels and organogels as vehicles for cosmetic active ingredients. Journal of Cosmetic Science, 60, 627–636. https://doi.org/10.1111/j.1468-2494.2010.00580_4.x

Ojijo, N. K. O., Neeman, I., Eger, S., & Shimoni, E. (2004). Effects of monoglyceride content, cooling rate and shear on the rheological properties of olive oil/monoglyceride gel networks. Journal of the Science of Food and Agriculture, 84(12), 1585–1593. https://doi.org/10.1002/jsfa.1831

Pal, A., Shibu A., Michael A. R,, Joykrishna D., and Richard G. W. (2013). Comparison of Dipolar, H-Bonding, and Dispersive Interactions on Gelation Efficiency of Positional Isomers of Keto and Hydroxy Substituted Octadecanoic Acids. Langmuir 29 (21): 6467–75. https://doi.org/10.1021/la400664q.

Patel, A. R., Babaahmadi, M., Lesaffer, A., & Dewettinck, K. (2015). Rheological Profiling of Organogels Prepared at Critical Gelling Concentrations of Natural Waxes in a Triacylglycerol Solvent. Journal of Agricultural and Food Chemistry, 63(19), 4862–4869. https://doi.org/10.1021/acs.jafc.5b01548

Perez-Nowak V., inventor; L´Oreal S. A., assignee . Fluid cosmetic composition, useful for making up and/or caring the skin and/or lips, comprises polyester, non-volatile silicone oil, organogelling agent comprising N-acylglutamides e.g. N-

lauroylglutamic acid dibutylamide, and wax. France patent FR2975296A1 (2012). https://patents.google.com/patent/FR2975296A1/en?oq=FR+Patent+2975296+A1

Rocha-Amador, O. G., Gallegos-Infante, J. A., Huang, Q., Rocha-Guzman, N. E., Rociomoreno-Jimenez, M., and Gonzalez-Laredo, R. F. (2014). Influence of commercial saturated monoglyceride, mono-/diglycerides mixtures, vegetable oil, stirring speed, and temperature on the physical properties of organogels. International Journal of Food Science, 2014. https://doi.org/10.1155/2014/513641

Rogers, M. A., and Marangoni, A. G. (2008). Non-isothermal nucleation and crystallization of 12-hydroxystearic acid in vegetable oils. Crystal Growth and Design, 8(12), 4596–4601. https://doi.org/10.1021/cg8008927

Rogers, M. A., Strober, T., Bot, A., Toro-Vazquez, J. F., Stortz, T., and Marangoni, A. G. (2014). Edible oleogels in molecular gastronomy. International Journal of Gastronomy and Food Science, 2(1), 22–31. https://doi.org/10.1016/j.ijgfs.2014.05.001

Sagiri, S. S., Singh, V. K., Pal, K., Banerjee, I., and Basak, P. (2015). Stearic acid based oleogels: A study on the molecular, thermal and mechanical properties. Materials Science and Engineering C, 48, 688–699. https://doi.org/10.1016/j.msec.2014.12.018

Toro-Vazquez, J. F., Morales-Rueda, J. A., Dibildox-Alvarado, E., Charó-Alonso, M.A., Alonzo-Macias, M., and González-Chávez, M. M. (2007). Thermal and textural properties of organogels developed by candelilla wax in safflower oil. JAOCS, Journal of the American Oil Chemists' Society, 84(11), 989–1000. https://doi.org/10.1007/s11746-007-1139-0

Toro-Vazquez, J. F., Mauricio-Pérez, R., González-Chávez, M. M., Sánchez-Becerril, M., Ornelas-Paz, J. de J., and Pérez-Martínez, J. D. (2013). Physical properties of organogels and water in oil emulsions structured by mixtures of candelilla wax and monoglycerides. Food Research International, 54(2), 1360–1368. https://doi.org/10.1016/j.foodres.2013.09.046

Toro-Vazquez, J. F., Morales-Rueda, J., Torres-Martínez, A., Charó-Alonso, M. A., Mallia, V. A., and Weiss, R. G. (2013). Cooling rate effects on the microstructure, solid content, and rheological properties of organogels of amides derived from stearic and (R)-12- hydroxystearic acid in vegetable oil. Langmuir, 29(25), 7642–7654. https://doi.org/10.1021/la400809a

Toro-Vazquez, J. F., Rangel-Vargas, E., Dibildox-Alvarado, E., and. Charó-Alonso M.A. (2005). Crystallization of Cocoa Butter with and without Polar Lipids Evaluated by Rheometry, Calorimetry and Polarized Light Microscopy. European Journal of Lipid Science and Technology 107 (9): 641–55. https://doi.org/10.1002/ejlt.200501163.

Toro-Vazquez, J. F., and Pérez-Martínez, J. D. (2018). Thermodynamic Aspects of Molecular Gels, in Monographs in Supramolecular Chemistry, ed R. G. Weiss. (London, U. K. : Royal Society of Chemistry), 57–87. https://doi.org/10.1039/9781788013147-00057

Table 1. Lattice spacing (*d*) determined by X-ray diffraction (SAXS and WAXS region) and calculated extended molecular length (*L*) for the alkyl esters studied in neat powder.

	ALKYL ESTER	*d* (Å)		*L* [a] (Å)	Proposed packing arrangement	Predominant crystal shape
		SAXS region	WAXS region			
SYMMETRIC	14:14	44.64	12.43,4.54, 4.39, 4.30, 4.20, 4.09 3.80	36.93	Monoclinic	platelet
	16:16	52.02	14,15, 4.60, 4.29, 4.21, 4.11, 3.80	42.21	Monoclinic	platelet
	18:18	62.80	16.01, 4.34, 4.27, 4.21, 4.12, 3.80	47.48	Monoclinic	platelet
	20:20	71.83	17.79, 4.15, 3.73	52.76	Orthorhombic	platelet
	22:22	82.28	19.78, 4.23, 3.78	58.03	Orthorhombic	platelet
ASYMMETRIC	18:14	52.34 43.49	4.22, 3.80	42.21	Orthorhombic	acicular
	18:16	67.28	16.97, 4.24, 3.82	44.84	Orthorhombic	acicular
	18:20	67.28	17.04, 4.23, 3.81	50.16	Orthorhombic	acicular
	18.22	65.21	16.67, 4.23, 3.77	52.76	Orthorhombic	acicular

[a] The corresponding alkyl ester molecule was obtained using Chemdraw Ultra software (V. 12.0.2.1076; Cambridge Soft Corporation, USA), and then measured using Chem3D software (V. 17.1). In order to obtain the theoretical carbon-carbon length, in all cases we preserved the extended molecular configuration of the alkyl ester.

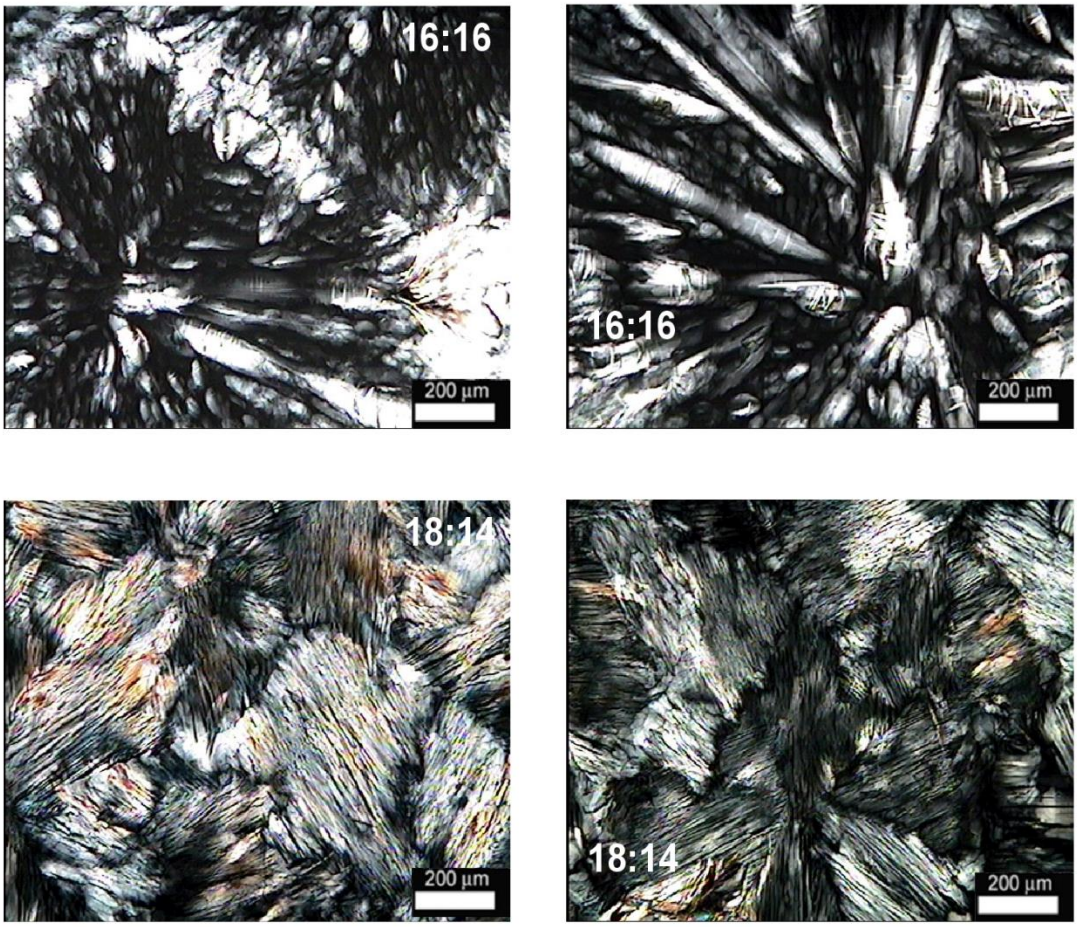

Figure 1. Polarized light microscopy for 60% (wt/wt) solutions in high oleic safflower oil of the symmetric (16:16) and asymmetric (18:14) alkyl esters. The same ester solution is presented at two levels of magnification.

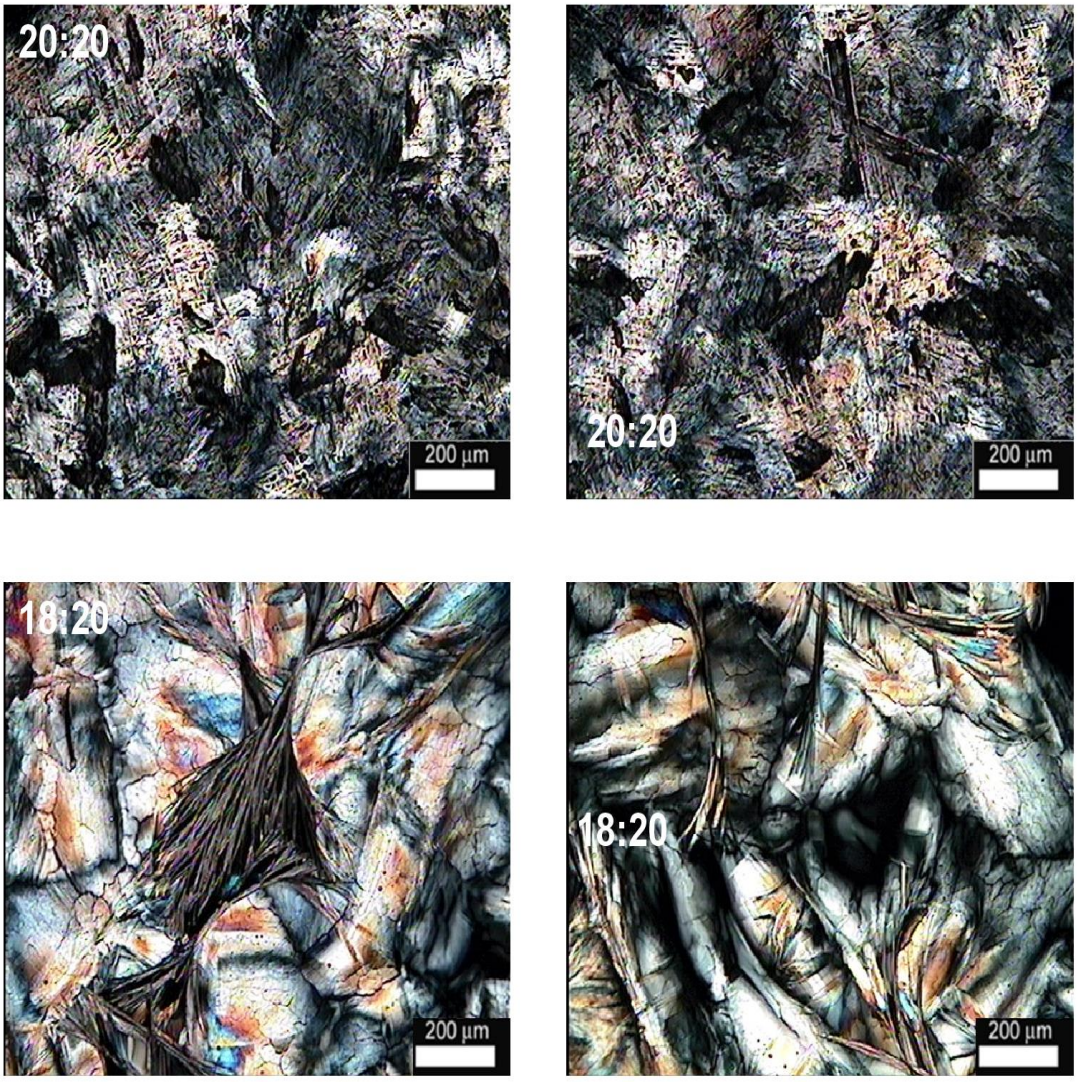

Figure 2. Polarized light microscopy for 60% (wt/wt) solutions in high oleic safflower oil of the symmetric (20:20) and asymmetric (18:20) alkyl esters. The same ester solution is presented at two levels of magnification.

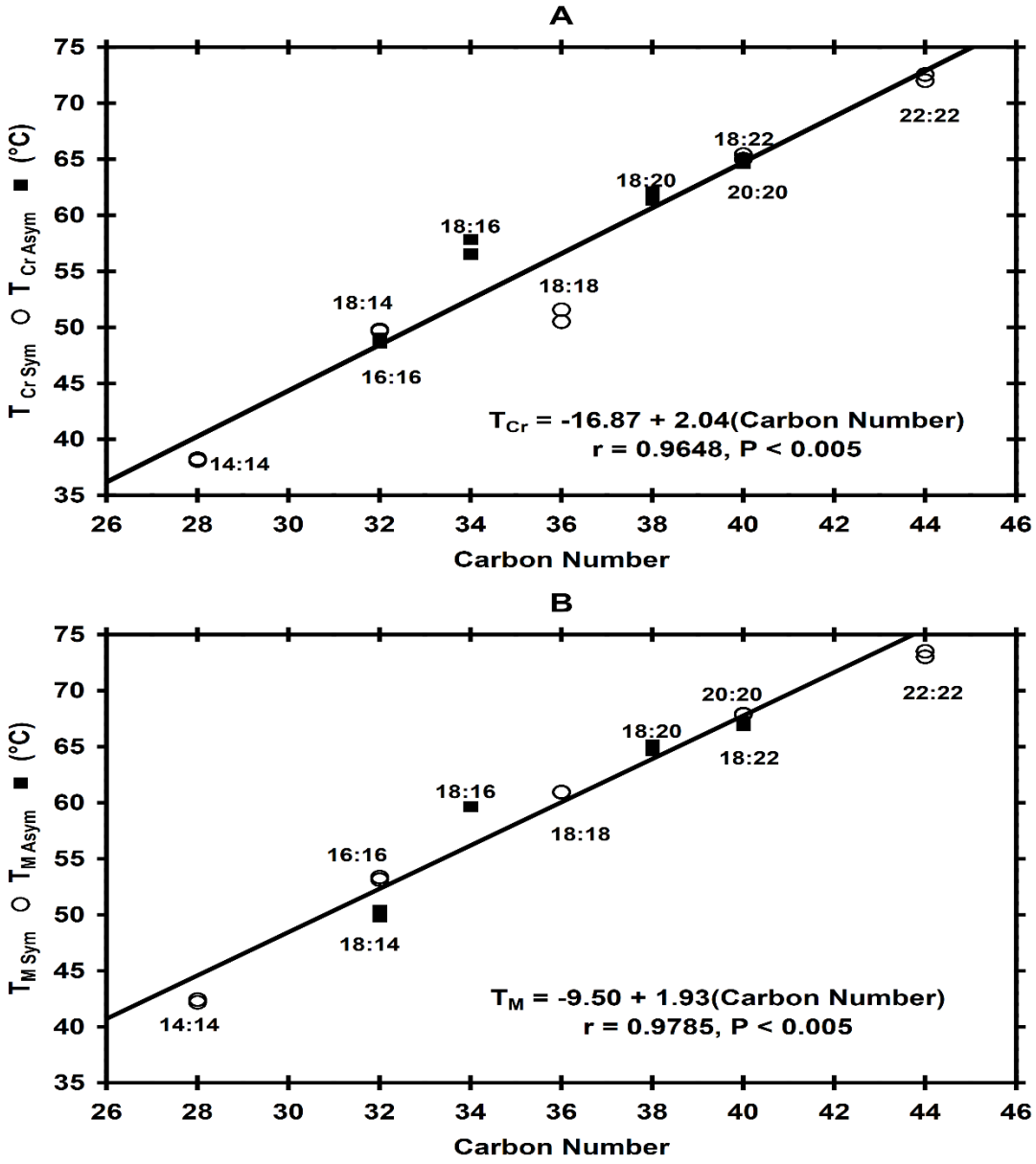

Figure 3. Crystallization (T_{Cr}) and melting (T_M) temperatures for the neat symmetric and asymmetric neat esters as a function of the carbon number of the alkyl esters. The equations show the linear regression of T_{Cr} (A) and T_M (B) as a function of the alkyl esters carbon number, the corresponding regression coefficient (r) and statistical significance (P).

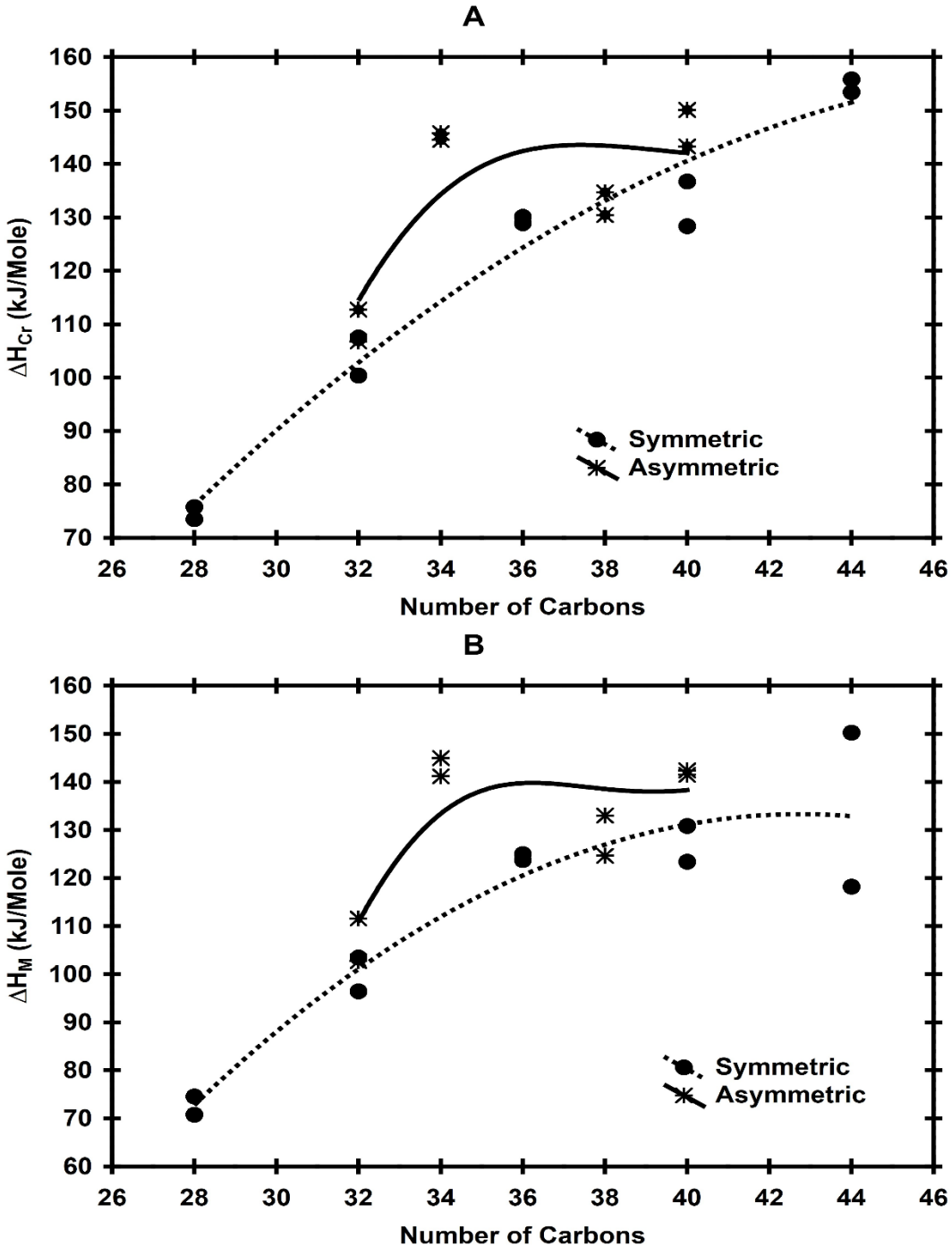

Figure 4. Heat of crystallization (ΔH_{Cr}; A) and melting (ΔH_M; B) for the neat symmetric and asymmetric esters as a function of the alkyl esters carbon number.

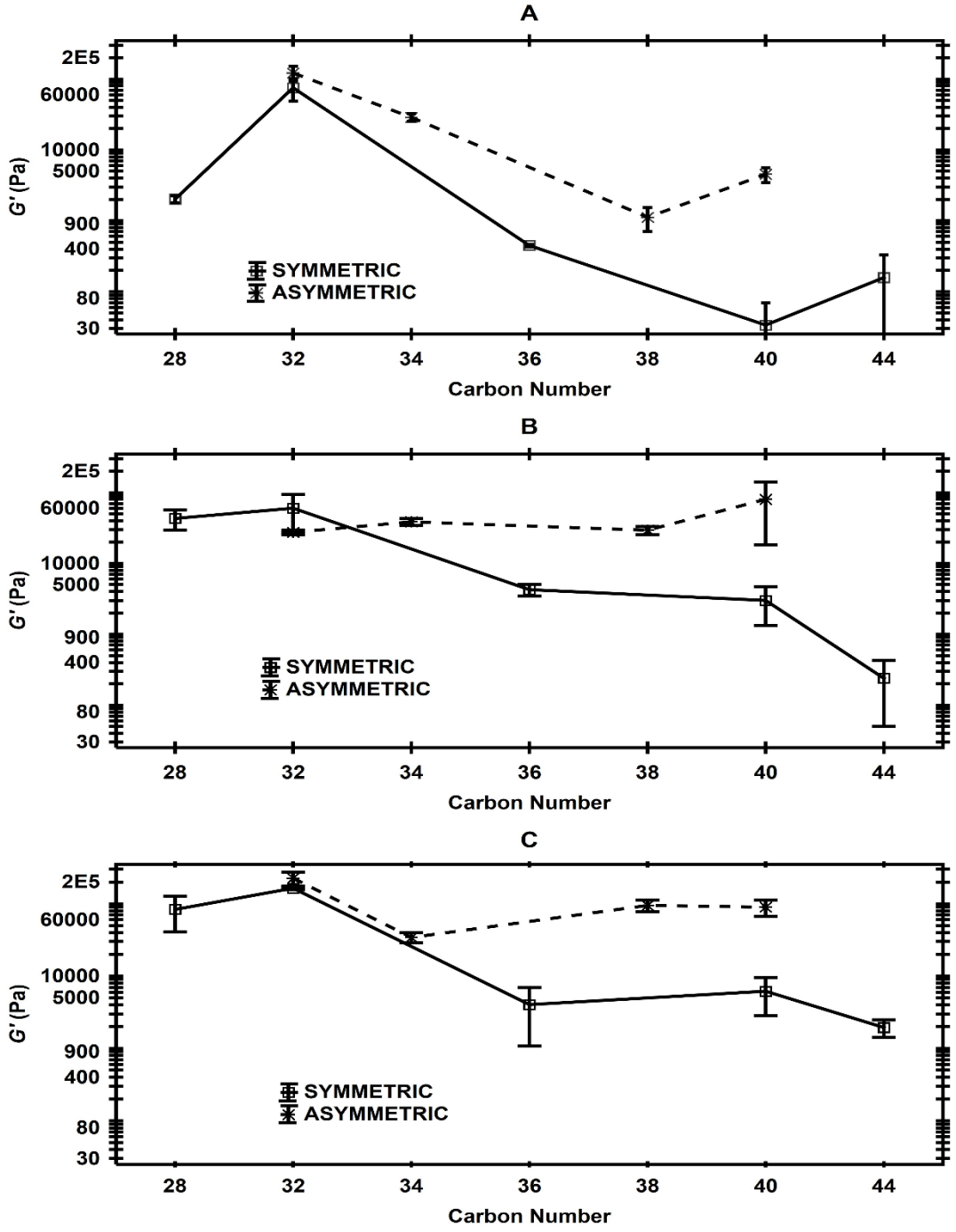

Figure 5. Elastic modulus (*G'*; -5°C) for the 3% (wt/wt) oleogels formulated with symmetric and asymmetric alkyl esters as a function of the carbon number of the esters. A, 0% MSG; B, 0.5% MSG; C, 1% MSG (wt/wt).

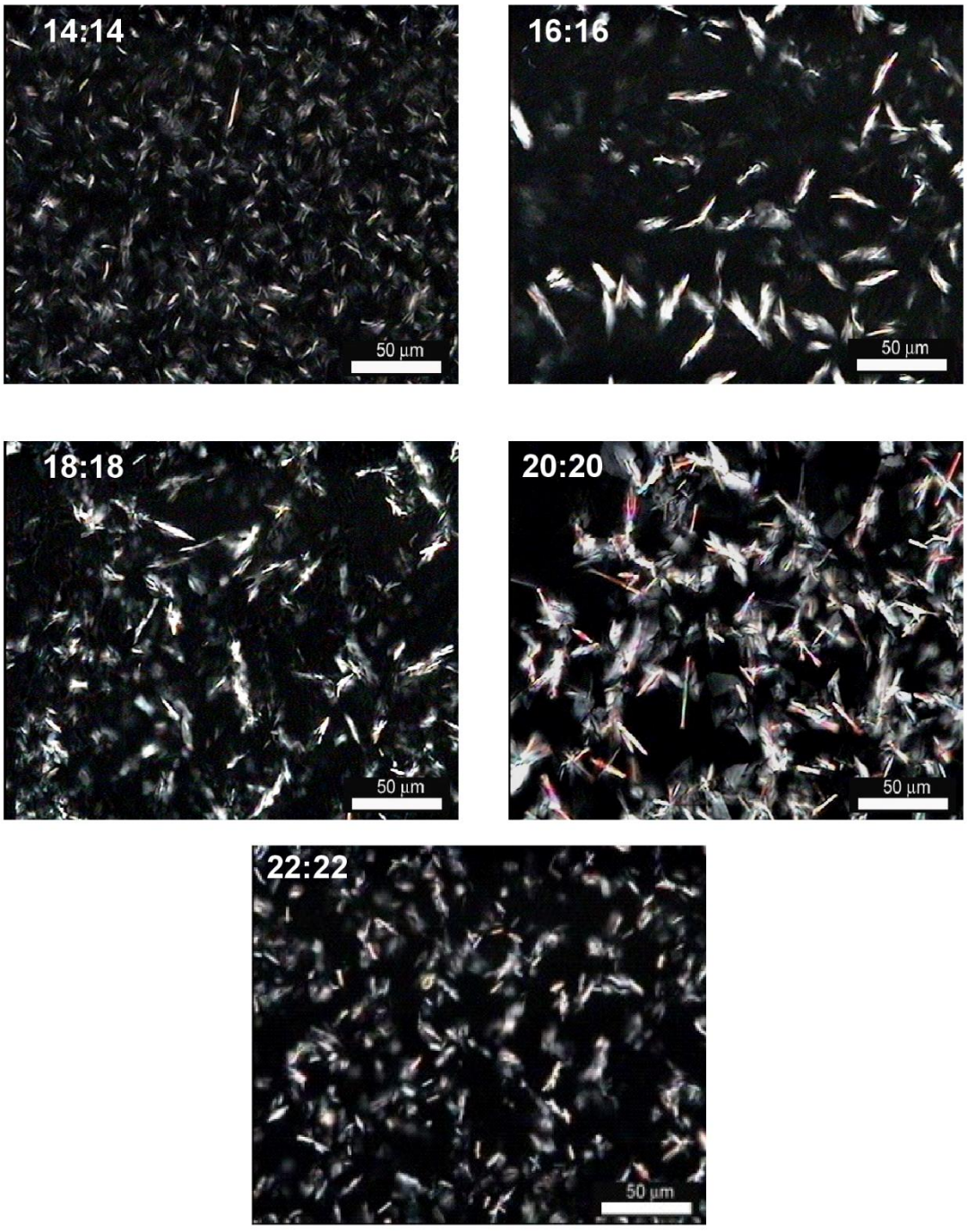

Figure 6. Polarized light microscopy (-5°C) for the 3% (wt/wt) oleogels in high oleic safflower oil formulated with the symmetric alkyl esters indicated and 0% MSG.

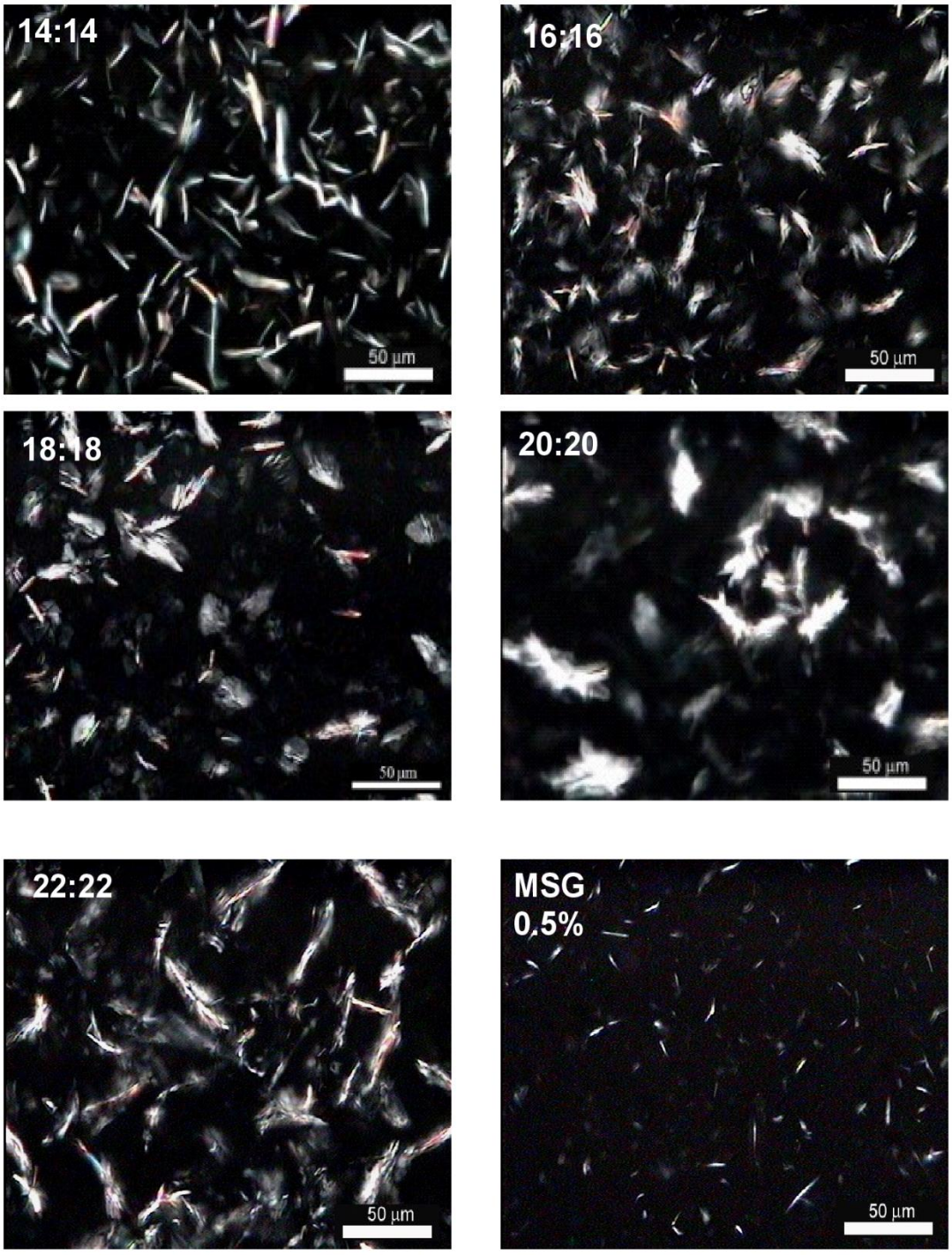

Figure 7. Polarized light microscopy (-5°C) for the 3% (wt/wt) oleogels in high oleic safflower oil formulated with the symmetric alkyl esters indicated and 0.5% MSG.

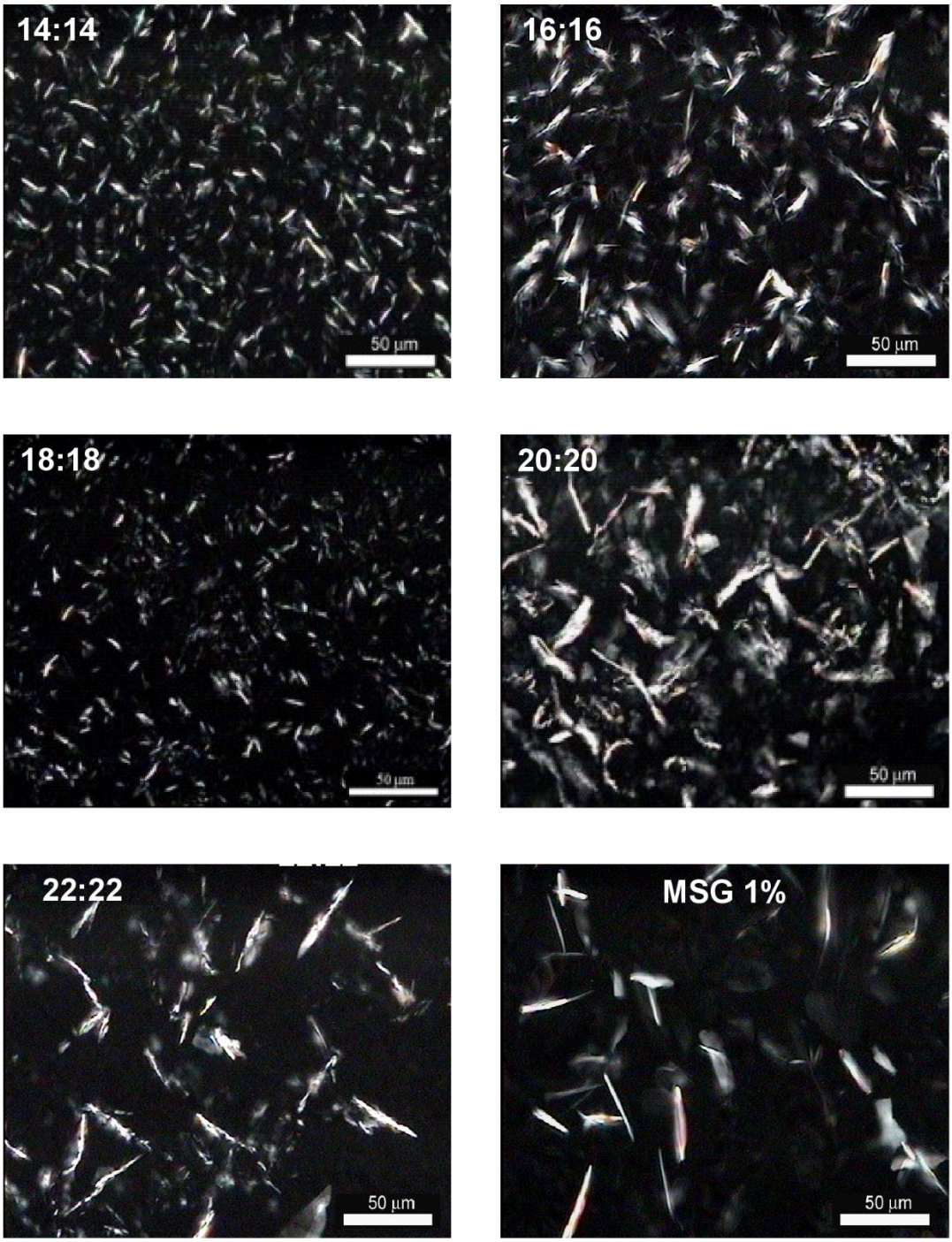

Figure 8. Polarized light microscopy (-5°C) for the 3% (wt/wt) oleogels in high oleic safflower oil formulated with the symmetric alkyl esters indicated and 1% MSG.

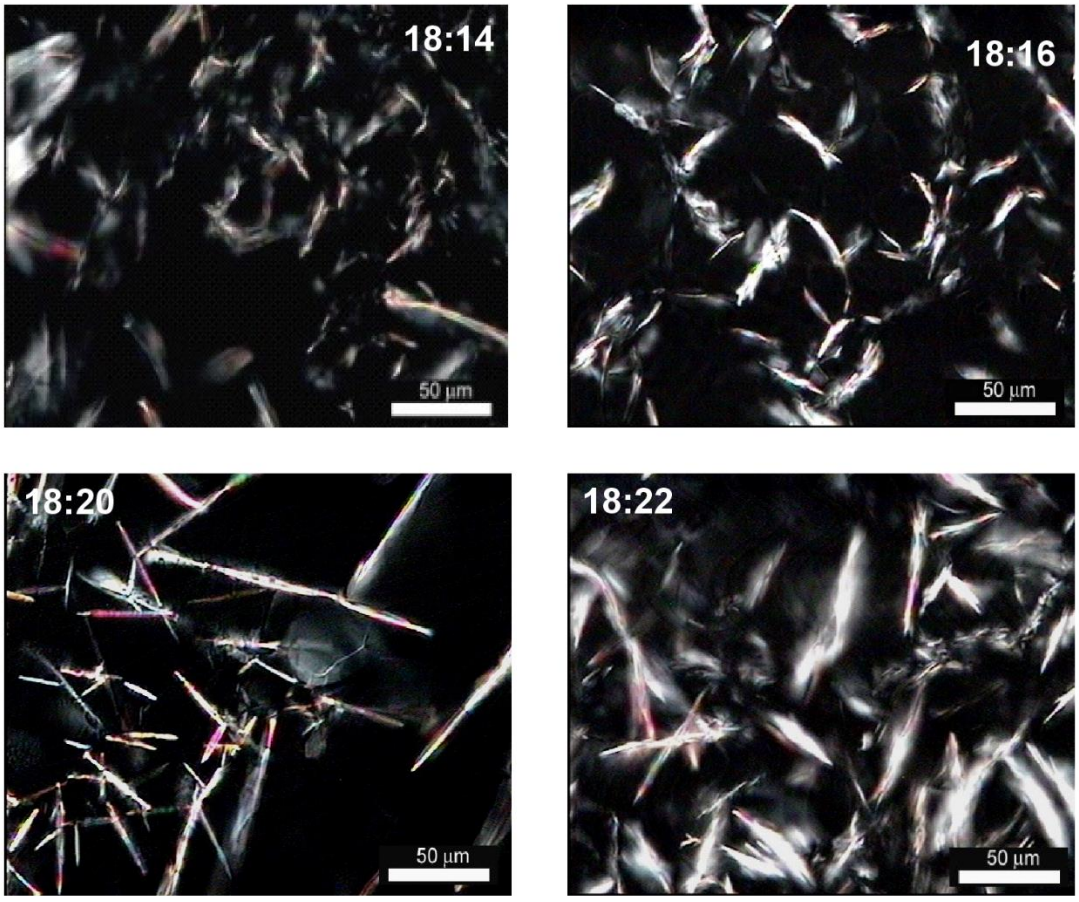

Figure 9. Polarized light microscopy (-5°C) for the 3% (wt/wt) oleogels in high oleic safflower oil formulated with the asymmetric alkyl esters indicated and 0% MSG.

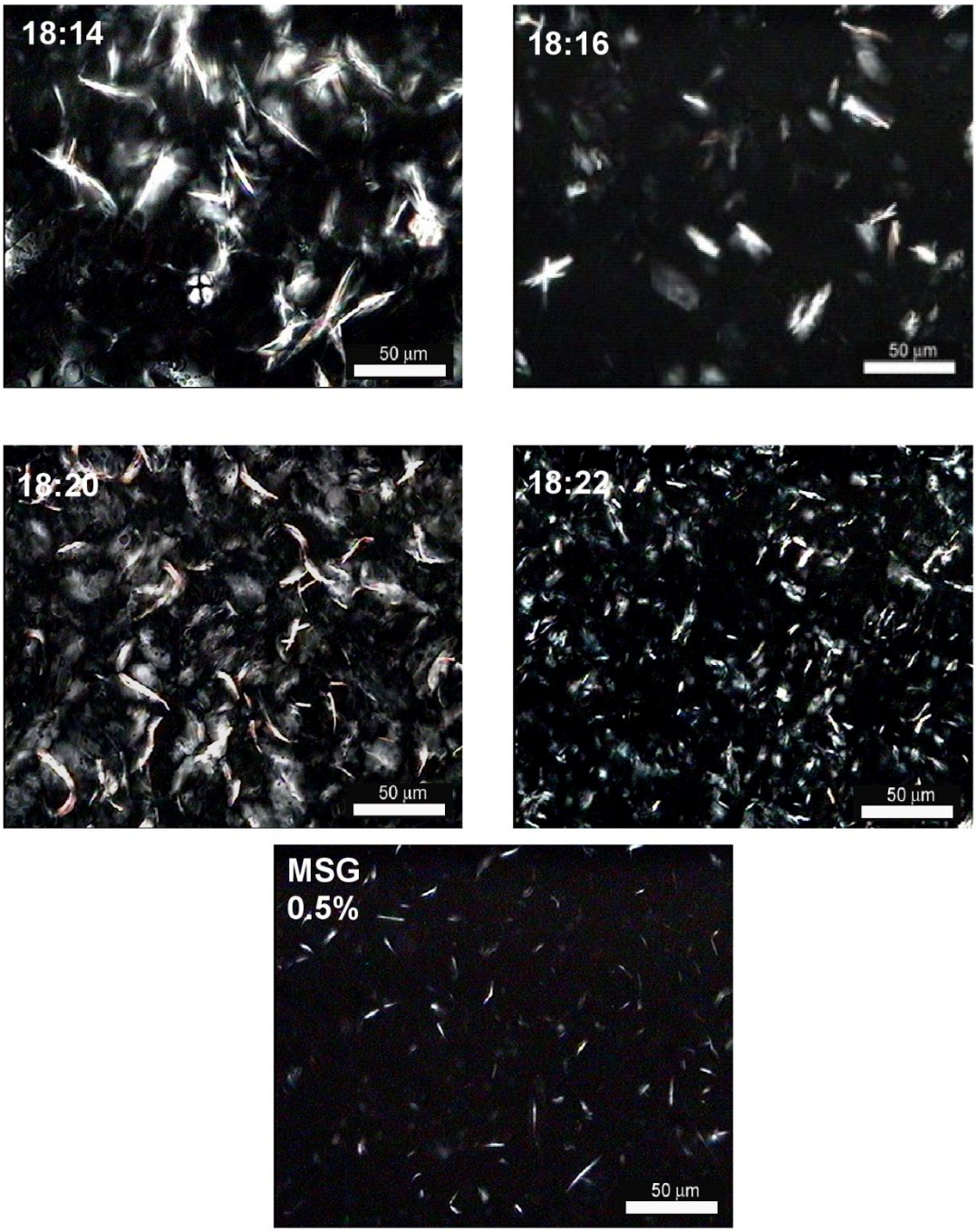

Figure 10. Polarized light microscopy (-5°C) for the 3% (wt/wt) oleogels in high oleic safflower oil formulated with the asymmetric alkyl esters indicated and 0.5% MSG.

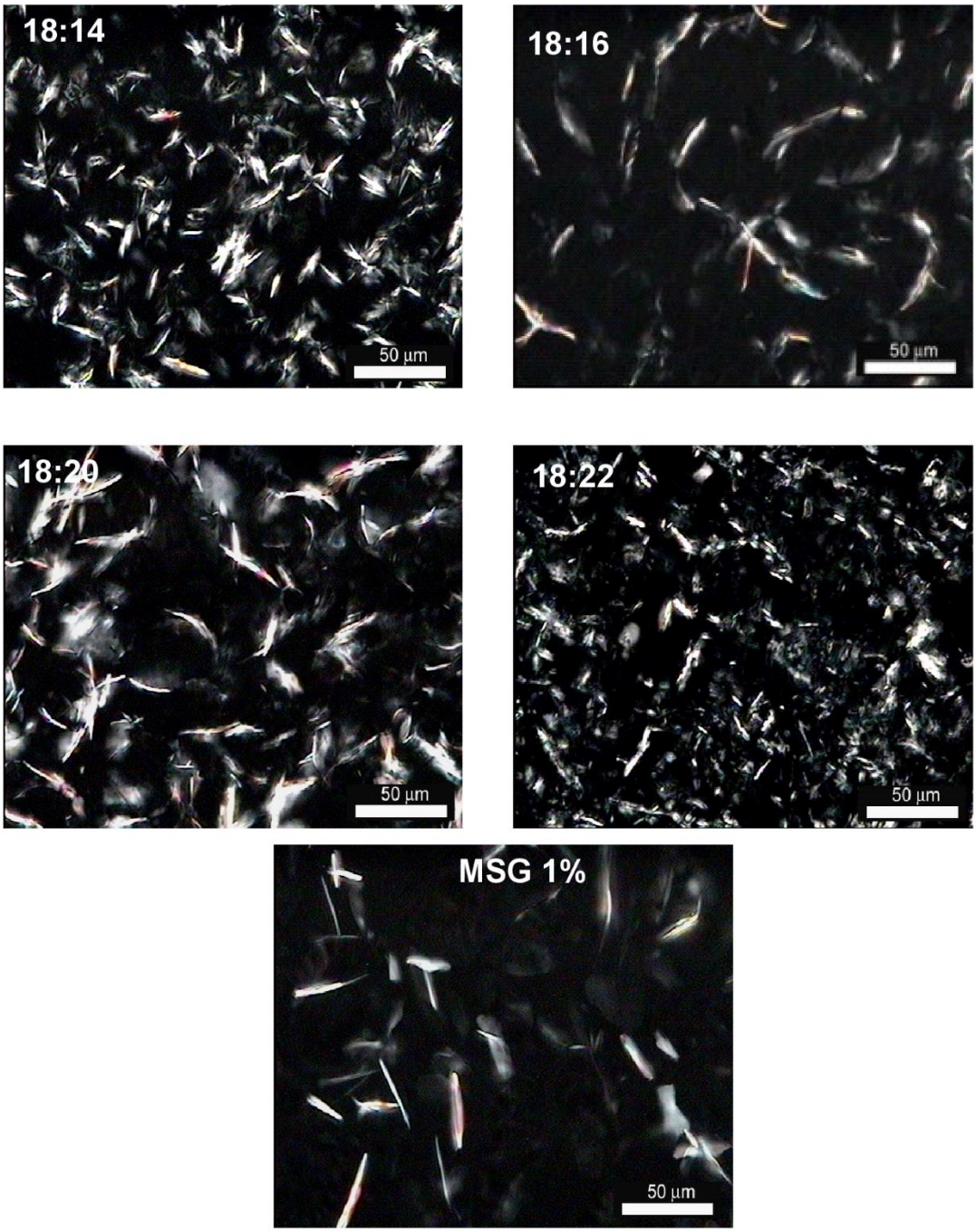

Figure 11. Polarized light microscopy (-5°C) for the 3% (wt/wt) oleogels in high oleic safflower oil formulated with the asymmetric alkyl esters indicated and 1% MSG.

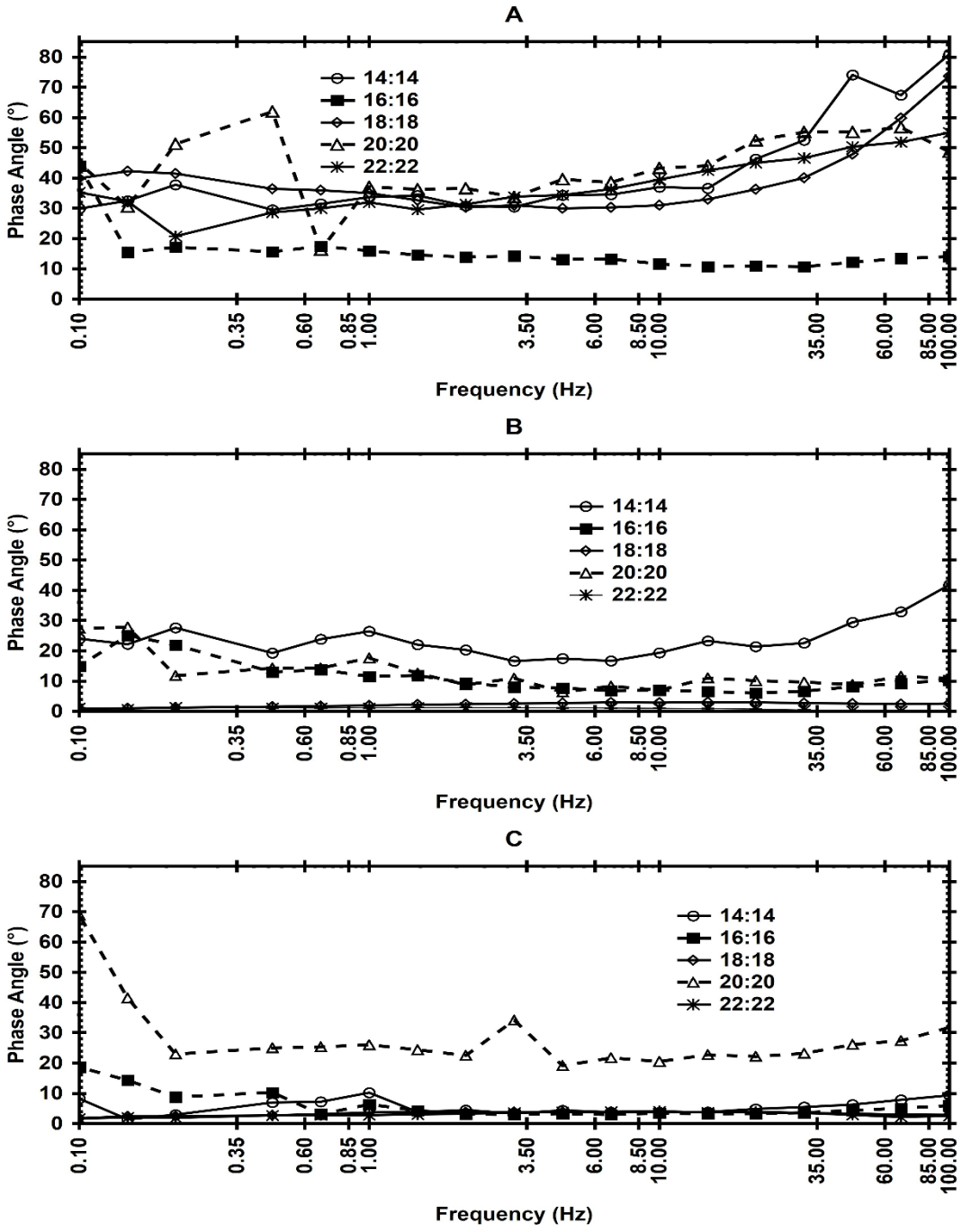

Figure 12. Frequency sweeps (-5°C) for the 3% (wt/wt) oleogels in high oleic safflower oil formulated with the symmetric alkyl esters indicated and: 0% MSG (A), 0.5% MSG (B), and 1% MSG (C).

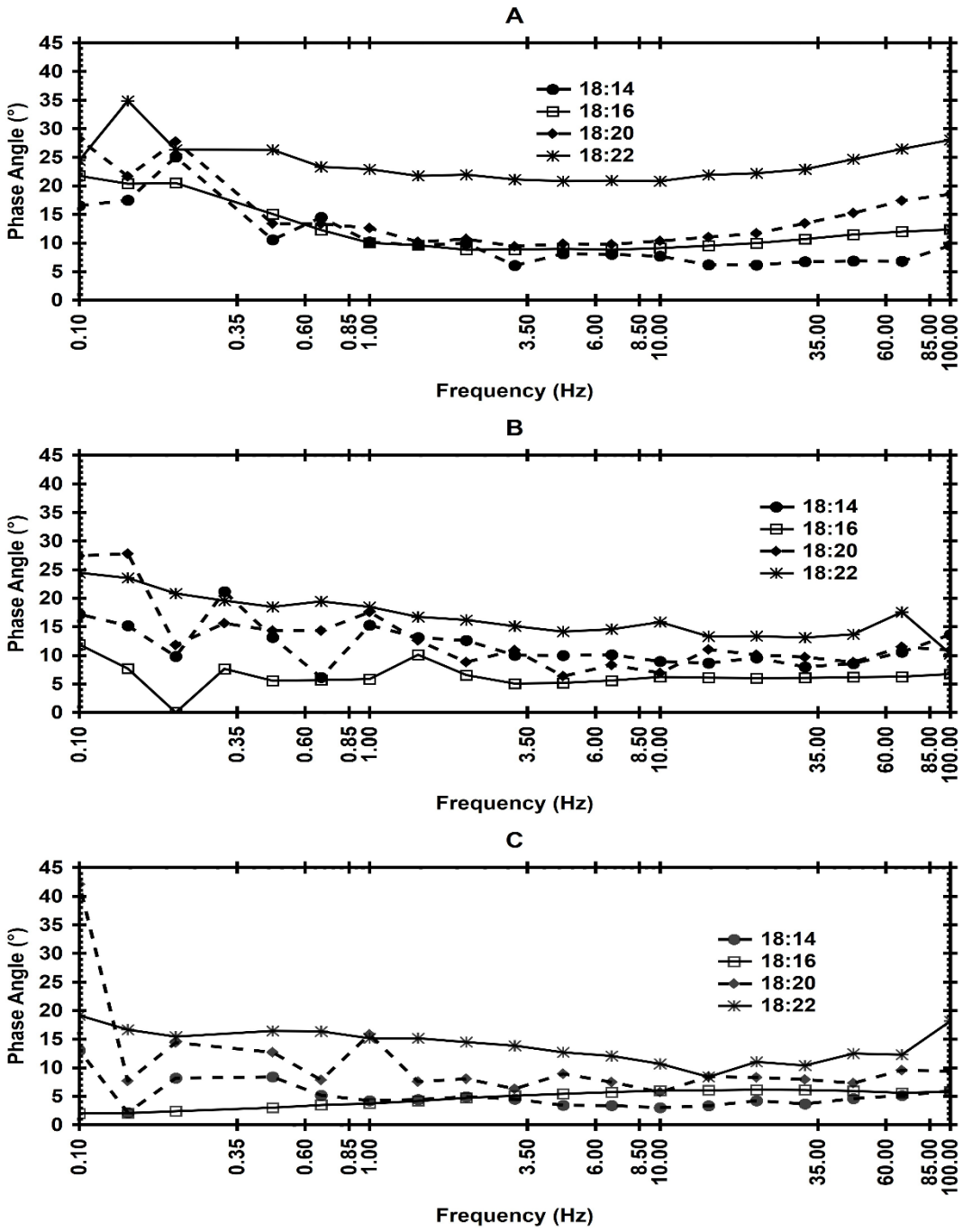

Figure 13. Frequency sweeps (-5°C) for the 3% (wt/wt) oleogels in high oleic safflower oil formulated with the asymmetric alkyl esters indicated and: 0% MSG (A), 0.5% MSG (B), and 1% MSG (C).

ANEXO 1

Información Complementaria del artículo (Supplementary Material)

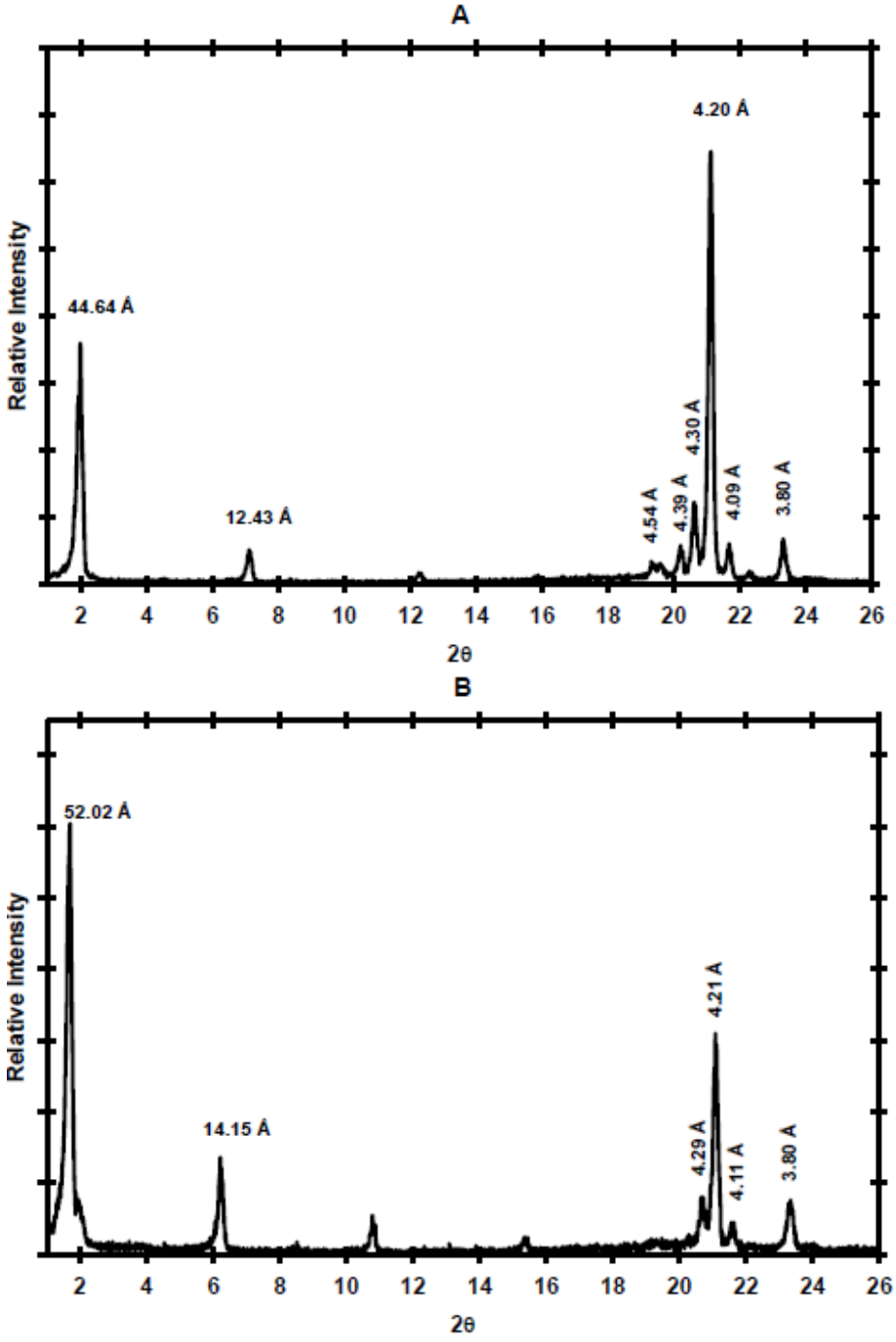

Figure 1SM. X-ray diffractograms (WAXS and SAXS) for the neat 14:14 (A) and 16:16 (B) esters.

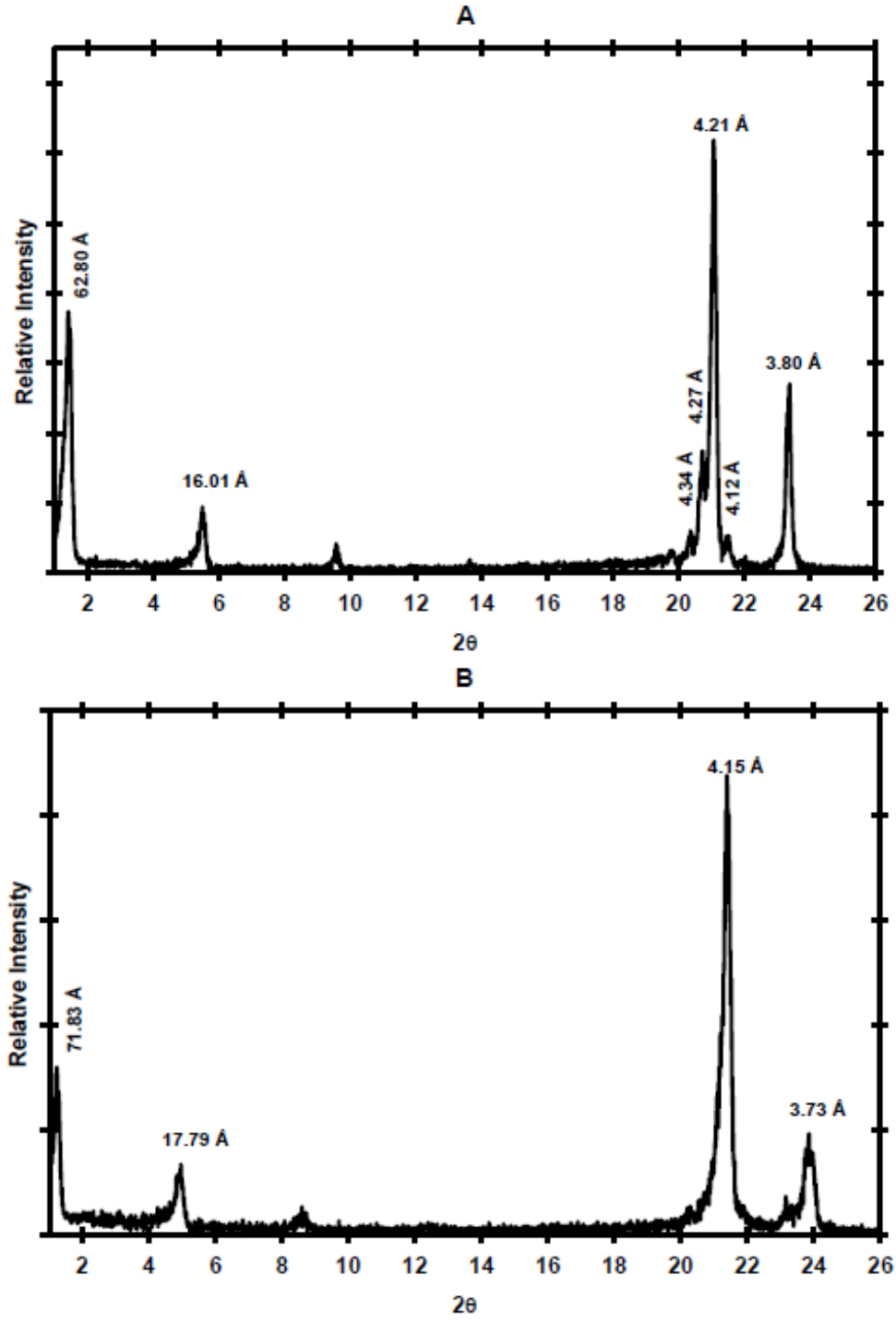

Figure 2SM. X-ray diffractograms (WAXS and SAXS) for the neat 18:18 (A) and 20:20 (B) esters.

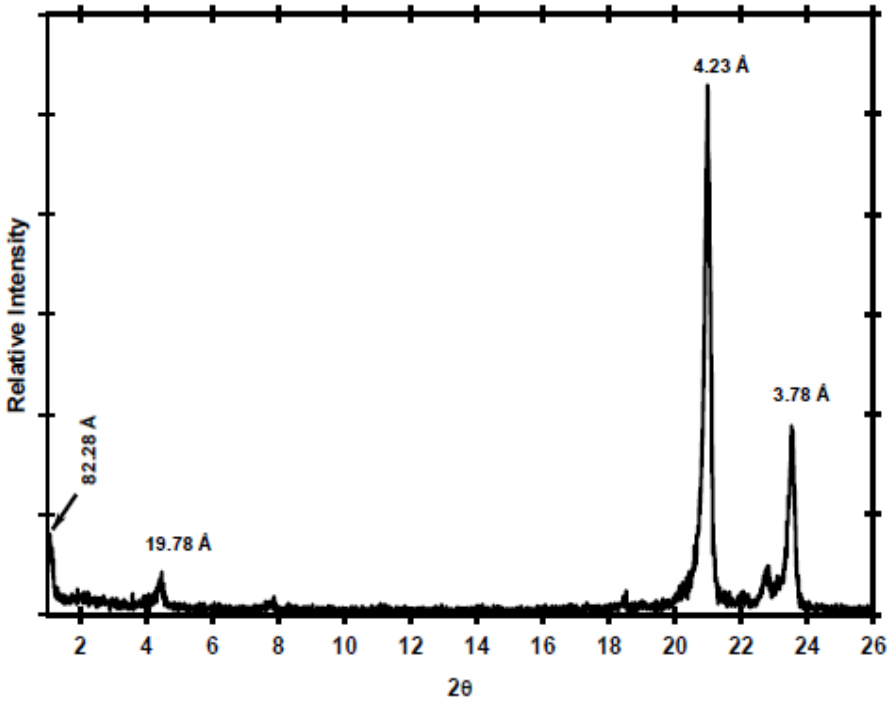

Figure 3SM. X-ray diffractogram (WAXS and SAXS) for the neat 22:22 ester.

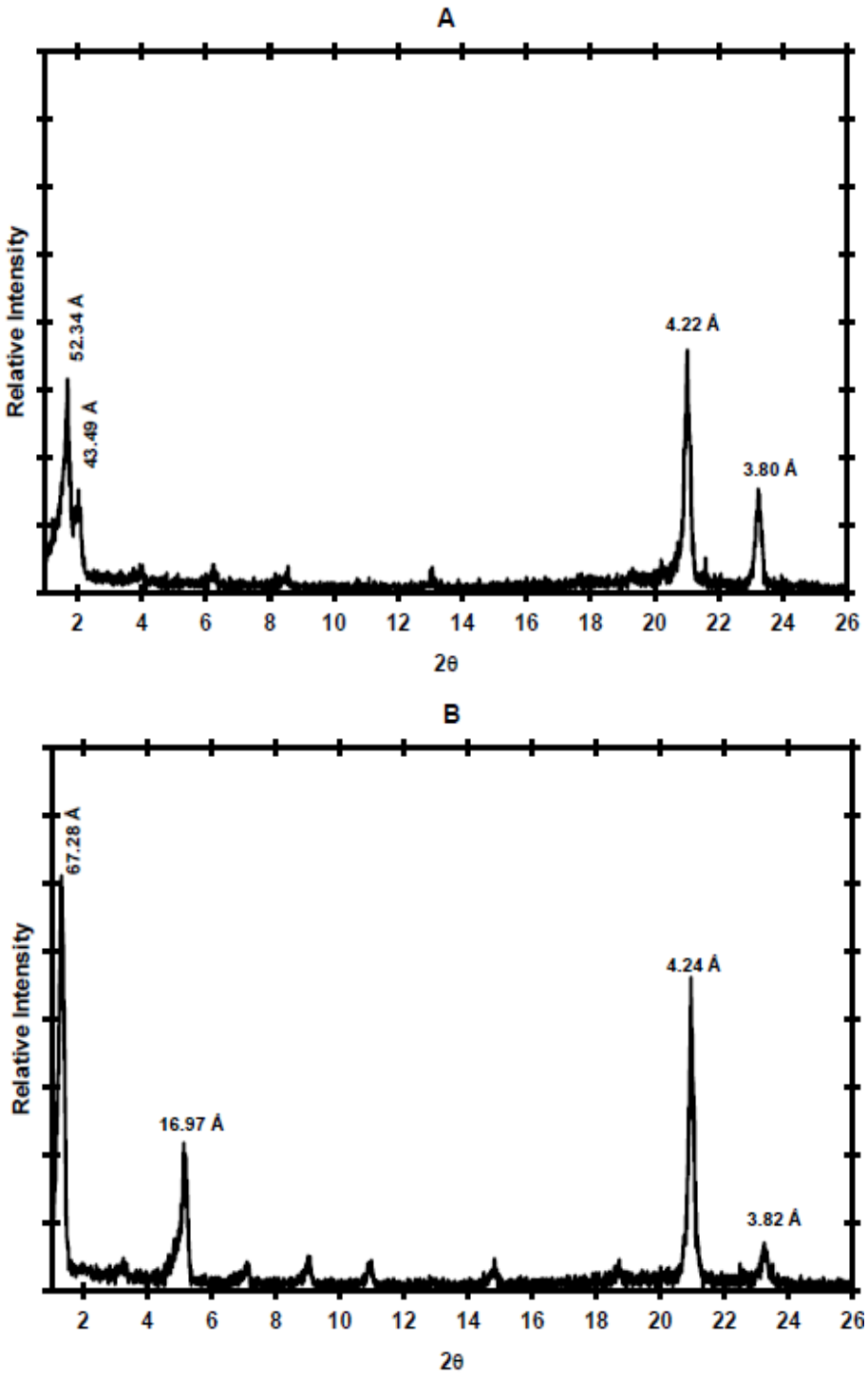

Figure 4SM. X-ray diffractograms (WAXS and SAXS) for the neat 18:14 (A) and 18:16 (B) esters.

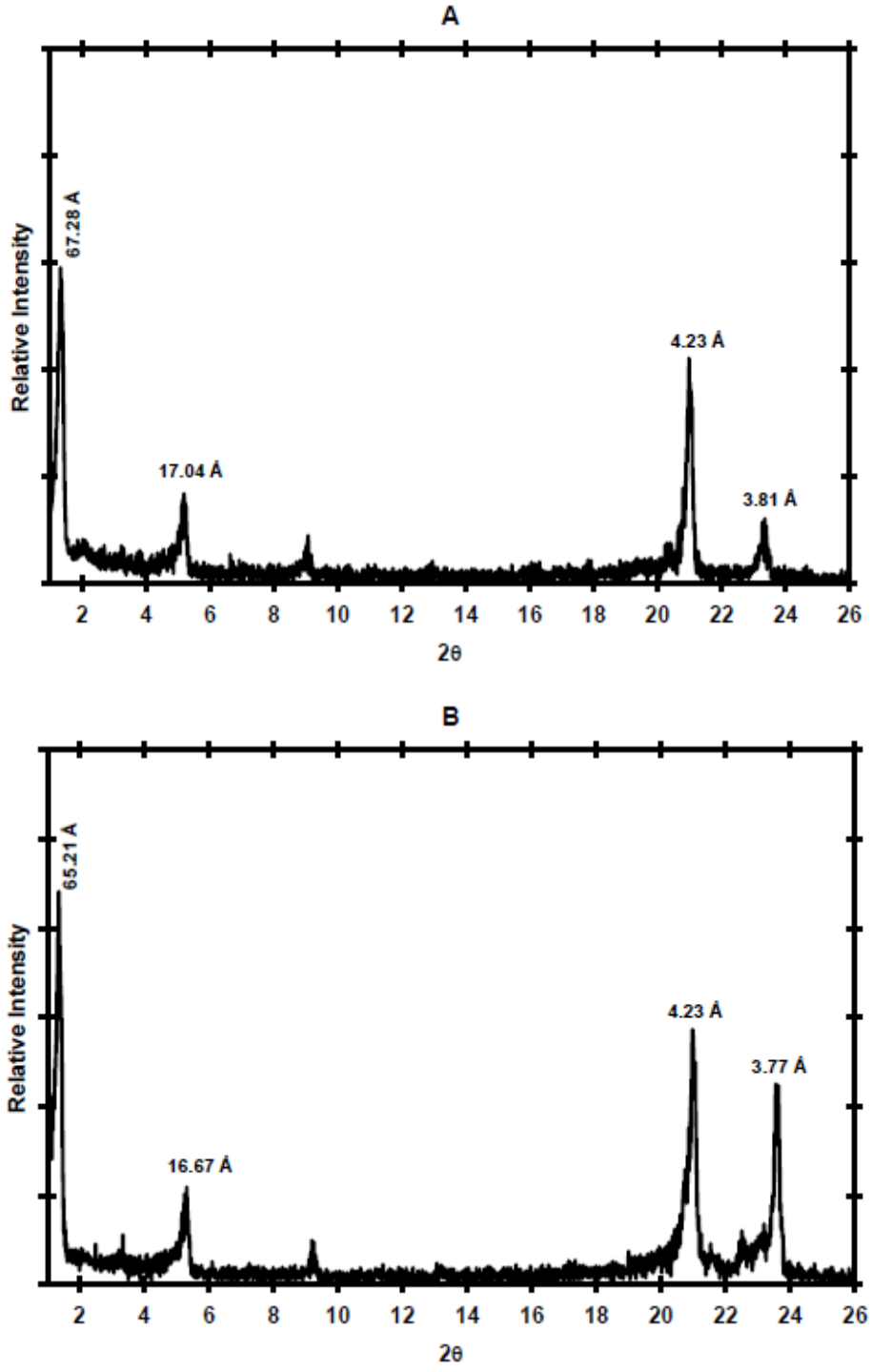

Figure 5SM. X-ray diffractograms (WAXS and SAXS) for the neat 18:20 (A) and 18:22 (B) esters.

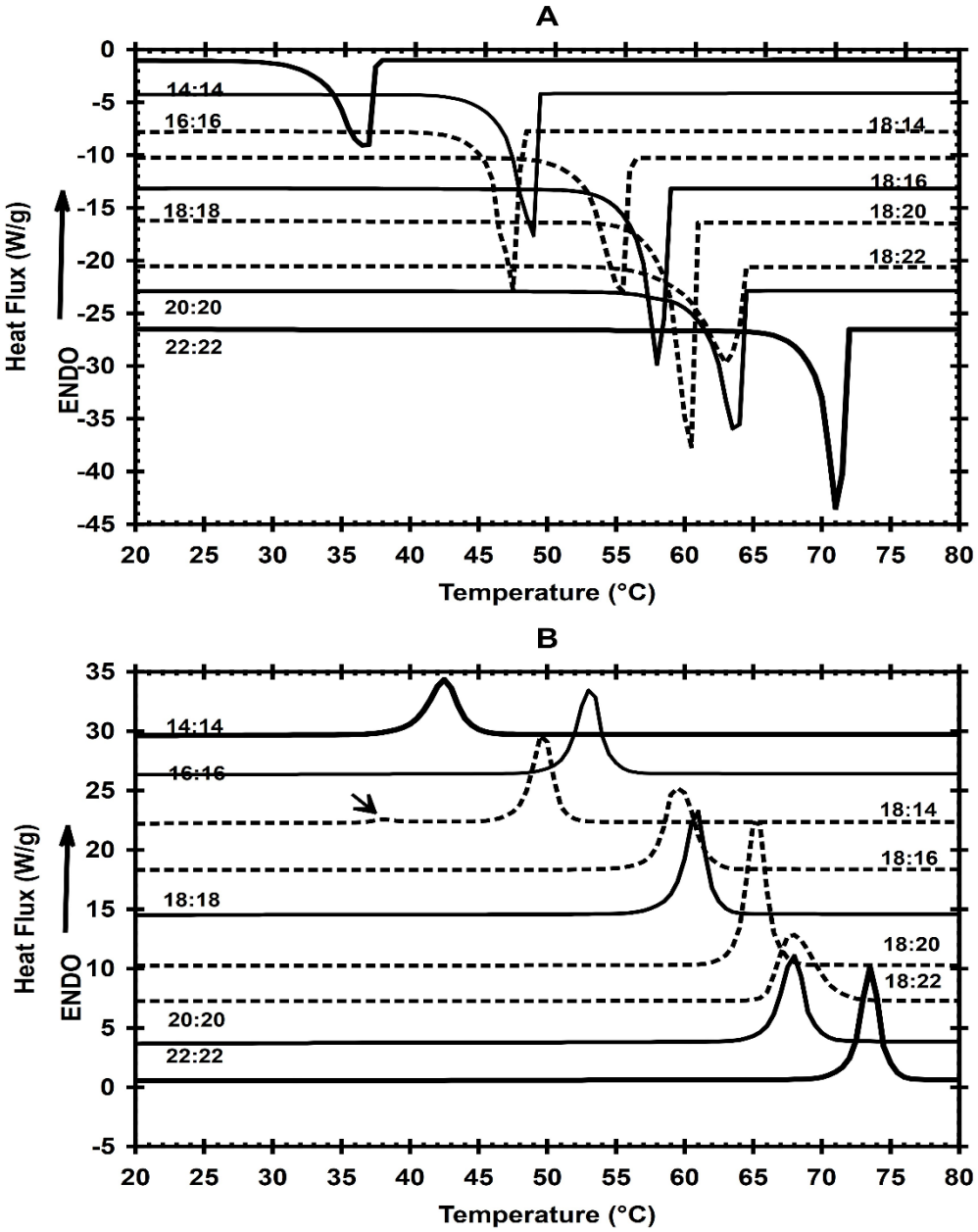

Figure 6SM. Crystallization (A) and melting (B) thermograms for the neat symmetric and asymmetric esters. The arrow in the melting thermograms (B) shows the small endotherm associated with one of the two polymorphs observed during melting of the 18:14 ester.

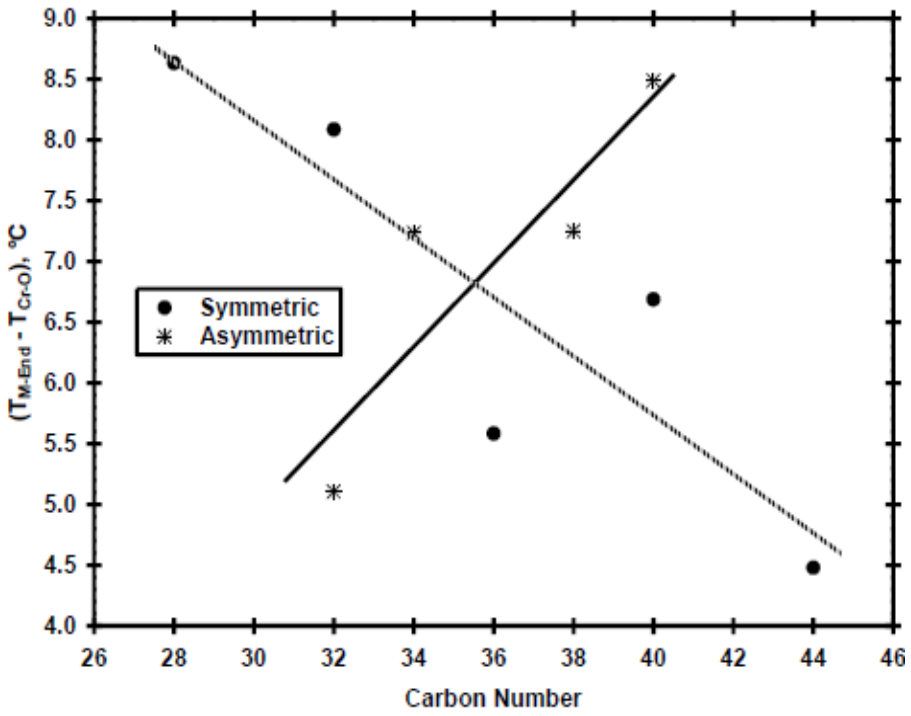

Figure 7SM. Relative supercooling ($T_{M\text{-}End}$ - $T_{Cr\text{-}O}$) for the 3% solutions of symmetric and asymmetric esters as a function of the alkyl esters' carbon number. The values reported correspond to the mean relative supercooling calculated from two independent measurements of $T_{M\text{-}End}$ and $T_{Cr\text{-}O}$ (n=2).

Table 1 SM. Parameters of the Hildebrand equation calculated for the symmetric and asymmetric alkyl ester solution in the vegetable oil through linear regression. The determination coefficient (r^2) and statistical significance of the corresponding linear regression are included.

	ALKYL ESTER	Hildebrand equation[a]		r^2	Statistical significance	Concentration (wt/wt) interval for alkyl ester solution[b]
		$1/T_E$	$R/\Delta H_M$			
SYMMETRIC	14:14	3.19	-0.093	0.9970	P < 0.01	3% and 6%
	16:16	3.02	-0.093	0.9876	P < 0.01	0.5% and 5
	18:18	2.96	-0.074	0.9471	P < 0.01	0.5% and 5
	20:20	2.92	-0.057	0.9953	P < 0.01	0.5% and 5
	22:22	2.91	-0.041	0.9051	P < 0.01	0.5% and 5
ASYMMETRIC	18:14	3.04	-0.095	0.9939	P < 0.01	0.5% and 5
	18:16	3.04	-0.06	0.9698	P < 0.01	0.5% and 5
	18:20	2.95	-0.062	0.9985	P < 0.01	0.5% and 5
	18:22	2.92	-0.061	0.9953	P < 0.01	0.5% and 5

[a] Equation 2 reported in section 2.3.2 of Materials and Methods.

[b] As indicated in section 2.3.2 of Materials and Methods, for each alkyl ester concentration of SE and AE we did at least three independent determinations ($n \geq 3$).

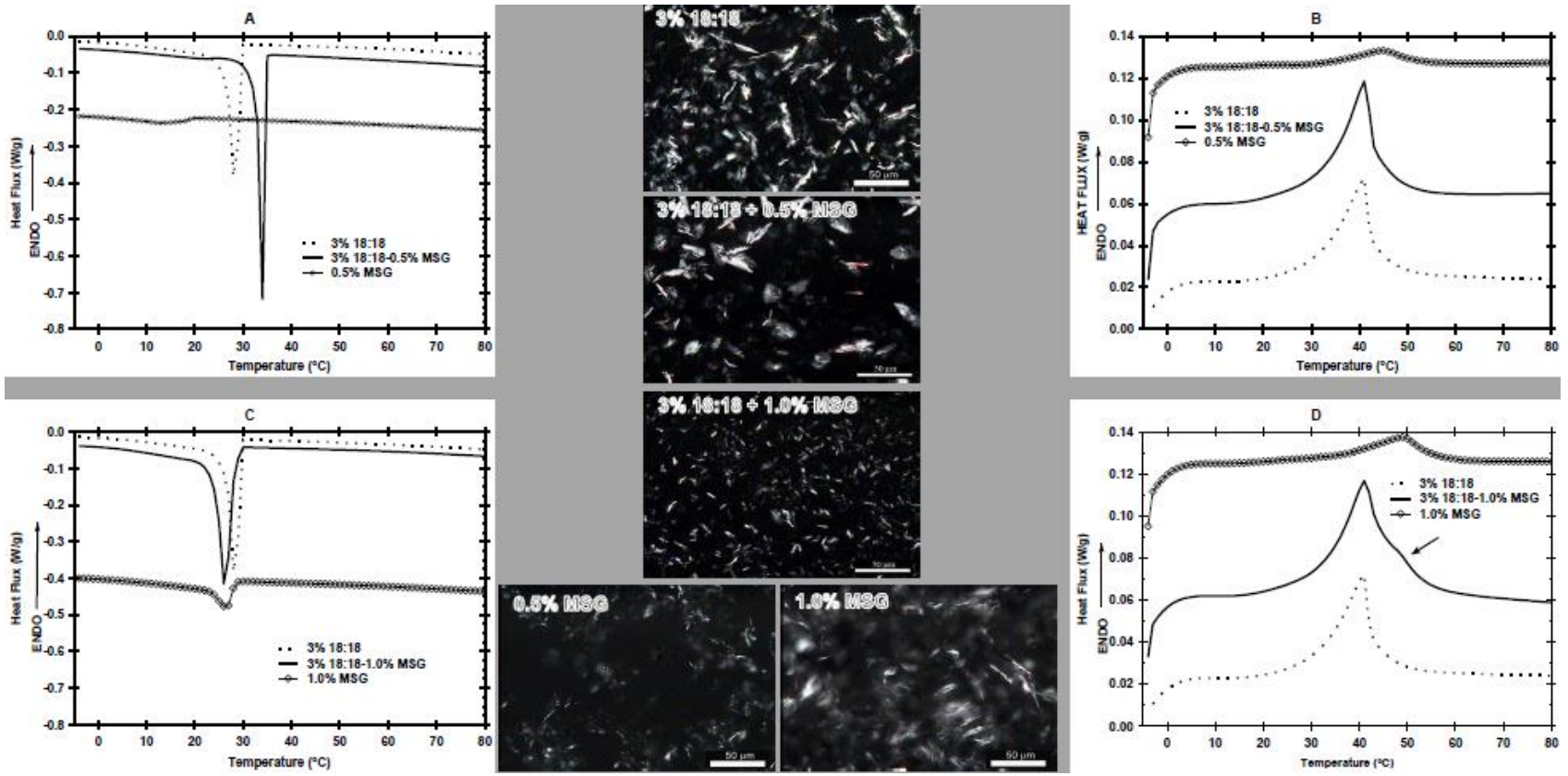

Figure 8SM. Cooling (A and C) and heating (B and D) thermograms for the 3% 18:18 oleogel with 0.5% MSG (A and B), and 1.0% MSG (C and D) in comparison with the 3% 18:18 oleogel (0% MSG) and the 0.5% and 1.0% MSG solution in the vegetable oil. The corresponding PLM at -5°C are included.

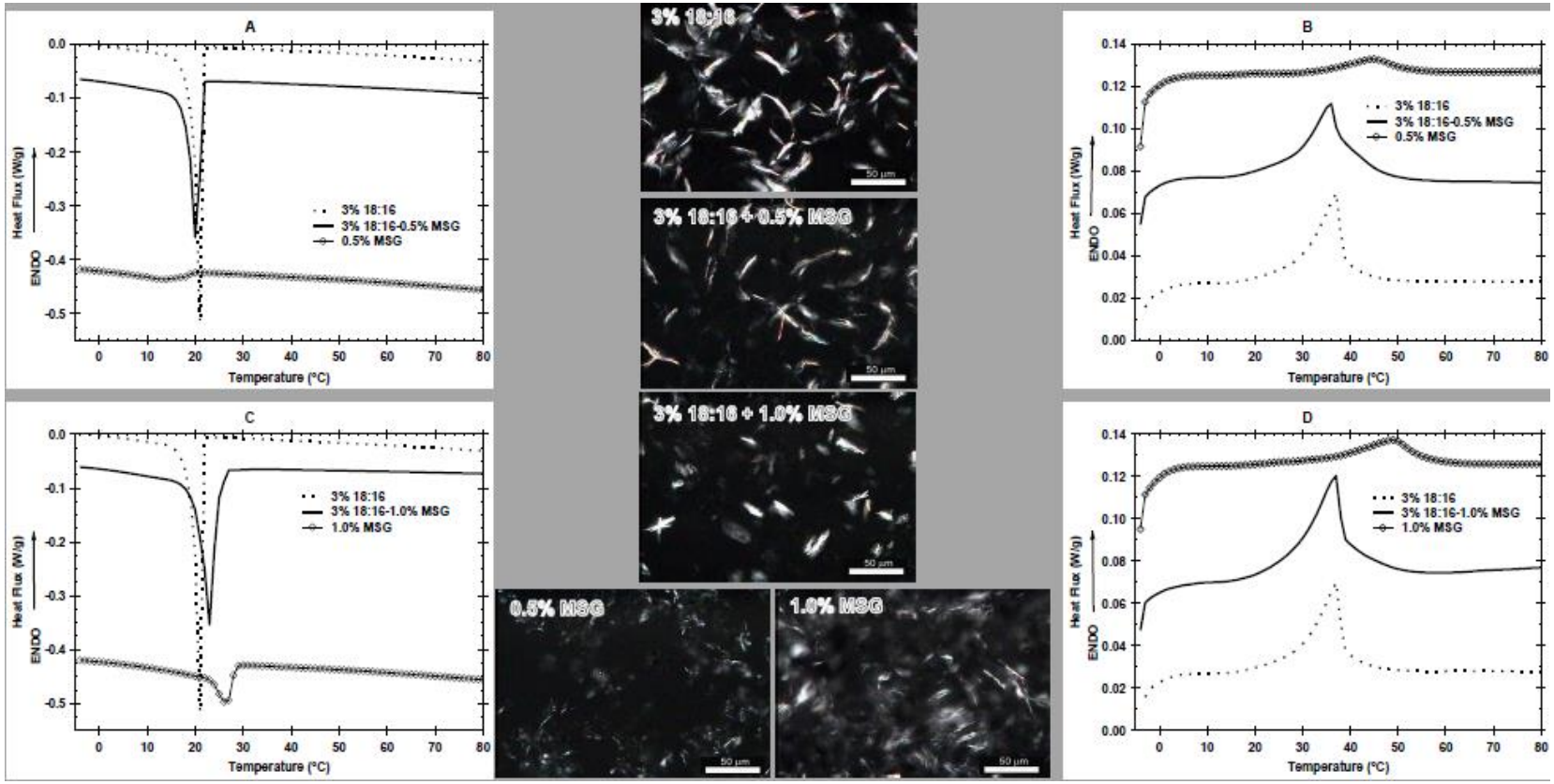

Figure 9SM. Cooling (A and C) and heating (B and D) thermograms for the 3% 18:16 oleogel with 0.5% MSG (A and B), and 1.0% MSG (C and D) in comparison with the 3% 18:18 oleogel (0% MSG) and the 0.5% and 1.0% MSG solution in the vegetable oil. The corresponding PLM at -5°C are included.

Table 2 SM. Melting temperature (T_M) of the 3% symmetric and asymmetric alkyl ester oleogels with 0%, 0.5% and 1% MSG. The results are reports as the mean and standard deviation of two independent measurements(*n*=2).

	ALKYL ESTER	3% ALKYL ESTER-0% MSG	3% ALKYL ESTER-0.5% MSG	3% ALKYL ESTER-1.0% MSG
		T_M (°C)	T_M (°C)	T_M (°C)
SYMMETRIC	14:14	17.34 [a] (0.03)	17.99 [a] (0.04)	17.98 [a] (0.25)
	16:16	31.12 [a] (0.37)	30.75 [a] (0.35)	31.21 [a] (0.13)
	18:18	40.08 [a] (0.24)	41.21 [b] (0.22)	41.13 [b] (0.06)
	20:20	49.69 [a] (0.52)	49.83 [a] (0.10)	49.68 [a] (0.52)
	22:22	55.14 [a] (0.13)	56.24 [b] (0.97)	56.13 [b] (0.64)
ASYMMETRIC	18:14	28.14 [a] (0.23)	27.92 [a] (0.11)	28.01 [a] (0.25)
	18:16	37.51 [a] (0.06)	36.64 [a] (0.31)	37.89 [a] (0.08)
	18:20	45.58 [a] (0.40)	45.61 [a] (0.81)	45.23 [a] (0.32)
	18:22	45.53 [a] (0.16)	48.19 [b] (0.01)	48.18 [b] (0.04)

[a, b] For the same alkyl ester T_M values with different subscript are statistically different ($P<0.05$), T_M values with the same subscript are statistically the same.

ANEXO 2

Tabla 1. Tamaño promedio de los cristales presentes en los oleogeles de esteres alquílicos (simétricos y asimétricos) y sus mezclas con 0.5% y 1% de monoglicérido. Mediciones realizadas a -5°C.

	3%Éster	Dimensión[a] (µm)	
		LONGITUD	ESPESOR
SIMÉTRICO	**14:14**	8.92 (2.52)	2.40 (0.73)
	14:14-0.5%MSG	24.26 (5.15)	4.58 (4.15)
	14:14-1%MSG	13.47 (7.30)	2.51(2.17)
	16:16	22.59 (6.30)	5.13 (1.03)
	16:16-0.5%MSG	22.81 (5.67)	3.80 (1.17)
	16:16-1%MSG	21.61 (7.38)	4.06 (1.51)
	18:18	23.09 (6.35)	2.97 (0.81)
	18:18-0.5%MSG	21.91 (3.57)	3.10 (0.73)
	18:18-1%MSG	12.74 (2.20)	2.77 (0.92)
	20:20	24.96 (3.50)	3.03 (0.80)
	20:20-0.5%MSG	79.07 (3.72)	15.19 (0.95)
	20:20-1%MSG	29.68 (6.56)	7.10 (1.94)
	22:22	14.65 (3.50)	2.20 (0.57)
	22:22-0.5%MSG	47.20 (5.65)	2.80 (1.08)
	22:22-1%MSG	36.46 (7.75)	3.37 (1.34)
ASIMÉTRICO	**18:14**	30.42 (7.94)	2.40 (0.84)
	18:14-0.5%MSG	36.44 (8.19)	3.08 (1.04)
	18:14-1%MSG	18.23 (5.60)	3.02 (0.97)
	18:16	29.99 (7.72)	3.76 (0.94)
	18:16-0.5%MSG	20.88 (4.05)	1.61 (0.56)
	18:16-1%MSG	26.93 (7.25)	2.75 (0.78)

	18:20	114.95 (38.76)	3.19 (1.26)
	18:20-0.5%MSG	21.44 (8.34)	5.11 (4.04)
	18:20-1%MSG	26.51 (6.52)	2.43 (1.13)
	18:22	115.40 (27.03)	3.66 (1.08)
	18:22-0.5%MSG	29.23 (9.55)	2.46 (0.95)
	18:22-1%MSG	35.00 (7.55)	3.30 (0.82)

[a] Datos obtenidos con el programa ImageJ. V1.53. Promedio y desviaciones estándar de mediciones realizadas en 10 cristales diferentes.